INNOVATION REPORT

The Development of a Laser-EMAT System Suitable for On-Line Inspection in the Continuous Casting Plant

Iain Baillie

April 2008

ABSTRACT

During the continuous casting process, both surface and internal defects can arise in the as-cast steel semi products, causing problems for downstream processes and customers[1]. These problems could be minimised if the steel could be inspected on-line, during the manufacturing process, whereby a feedback control system could be developed to alert operators should any defects arise and modifications need to be made to the process. The main benefit of on-line inspection is reducing operating costs. Additionally, the material flow through the mills and to the customer could be streamlined and optimised to ensure that defective or out of tolerance material is not sent through additional, expensive, value added processes[2,3]. The problem is that steel in the caster is at temperatures in excess of 800 °C and the environment is so harsh that most inspection technologies will not work under these conditions.

A review of the literature was conducted to assess technologies that could be applied to inspect the surface and internal quality of hot, moving steel within the harsh environment of a continuous caster[4]. This review enabled a non-contact ultrasonic technique to be selected, as this was suitable for the hostile environment and could find both internal and surface defects at the same time[4]. A further literature study was undertaken which showed that a Laser-EMAT (ElectroMagnetic Acoustic Transducer) system could be suitable for the application[5]. This technology uses a high energy, pulsed laser beam to generate ultrasound in the steel and non-contact EMATs to detect the ultrasonic signals. As this technology was not available off-the shelf, significant research needed to be conducted and ultrasonic experiments to find defects at room temperature and hot, moving steel were carried out[6].

The innovations and main results from important trials conducted as part of this project are included in this Innovation Report. Detailed research and development work, undertaken as part of this project can be found in the 'Steps towards an automated prototype system for inspecting hot, moving steel' portfolio submission[6]. The main achievement for this project is the creation of a prototype Laser-EMAT system that could find defects in moving steel, in excess of 800 °C.

ACKNOWLEDGEMENTS

Corus R, D & T

Mr P Griffith (Researcher):
All LabVIEW work presented in this report was programmed by Peter who followed my software specifications and who helped to take measurements with me.

Mr I Jones (Technician), Mr B Barry (Fitter) and Mr R Goater (Drawing Officer):
These people helped me to design and build numerous EMATs and EMAT holders and offered invaluable assistance installing apparatus both at Teesside and Swinden Technology Centres.

Dr A S Normanton (Manager), Mr A Scholes, Mr B Patrick:
For supporting me on my EngD.

The University of Warwick

Dr S Dixon (Senior Lecturer):
Explained Laser-EMAT technology to me and was my mentor throughout this project.

Dr X Jian (Research Assistant):
Conducted measurements on steel samples for finding internal defects using an EMAT-EMAT system. Used Finite Element Models to compare the theory against my practical measurements.

Mr J Reed (Technician) and Dr M Potter (Research Assistant):
Constructed EMAT pre-amplifiers.

CONTENTS

1. INTRODUCTION 1
2. THE CONTINUOUS CASTING PROCESS 3
3. THE IMPORTANCE OF ON-LINE INSPECTION TO REDUCING COSTS 6
3.1 Correcting Defects via Feedback Control during the Manufacturing Process 6
3.2 Reducing the Amount of Manual Inspection and Delays in the Slab Yard 6
3.3 Reducing the Costs Associated with Scarfing 7
4. HOW NON-CONTACT LASER-EMAT (ULTRASONIC) TECHNOLOGY WAS SELECTED BY REVIEWING THE LITERATURE 8
5. STEPS TAKEN TO DEVELOP AN ON-LINE SYSTEM 10
6. LASER-EMAT THEORY 11
6.1 The Laser Beam as a Broadband Ultrasonic Source 11
6.2 The EMAT as an Ultrasonic Receiver 11
6.3 How Surface waves can be used to Find Defects 12
6.4 How Bulk Waves Can be Used to Find Internal Defects 15
6.5 Optimising a Laser-EMAT System 16
7. DEVELOPMENT OF AN EMAT SENSOR CAPABLE OF WITHSTANDING TEMPERATURES GREATER THAN 1000 °C 17
7.1 Mechanisms that Affect Ultrasonic Signals when the Steel is Hot 17
7.2 Ultrasonic Experiments on Hot Steel Samples 20
7.3 Additional Tests and Results Conducted at High Temperature 24
7.4 Summary 29
8. DEVELOPMENT OF AN AUTOMATED INSPECTION SYSTEM 30
8.1 Construction of a Mechanical EMAT Holder to Accommodate Variability in Product Thickness 30
8.2 Constructing a New, Dedicated Data-logging PC 32
8.3 Construction of an Automated Trolley Inspection System 32
9. ON-LINE SURFACE DEFECT DETECTION ON HOT, MOVING STEEL 34
9.1 Experimental Method 34
9.2 How the Presence of a Surface Defect Can Affect Ultrasonic Signals 35
9.3 LabVIEW Controlled Trolley System to Inspect an Incrementally Moving Billet Sample at Room Temperature 36
9.4 Additional Tests to Move the Billet at a Constant Velocity 40
9.5 Pilot Rolling Mill System to Inspect a Moving Billet Sample at Room Temperature 41
9.6 Pilot Rolling Mill System to Inspect a Moving, Hot Billet Sample 41
9.7 Recommendations for Further Work to Improve Measurements at Elevated Temperature 43
10. DETECTING DEFECTS ON THE BOTTOM FACE OF THE BILLET, WITH THE LASER EMAT EQUIPMENT MOUNTED ON THE TOP FACE 44
11. LASER-EMAT ARRAYS 46
12. INSTALLATION ON THE PILOT PLANT CONTINUOUS CASTER 49
13. RECOMMENDATIONS FOR THE FINAL LASER-EMAT SYSTEM 53
14. MAIN INNOVATIONS 55
15. CONCLUSIONS 57
16. LIST OF PUBLISHED PAPERS RESULTING FROM THE ENGINEERING DOCTORATE PROJECT 58
17. REFERENCES 59

APPENDIX 1 63

1. INTRODUCTION

A schematic diagram showing an overview of this Engineering Doctorate project can be found in Fig. 1. This schematic shows the chronological progression of the work undertaken for this project and how the individual portfolio submissions were linked to one another and have been summarised for this Innovation Report.

Engineering Doctorate Submission Number 1 concluded that during the continuous casting process, both surface and internal defects can arise in steel products, causing problems for downstream processes and customers[1]. This submission illustrated how problems could be minimised if the steel could be inspected on-line, during the manufacturing process, whereby a feedback control system could be developed to alert operators should any defects arise thereby allowing them to make modifications to the process. The main benefit of on-line inspection is reducing operating costs. Additionally, the material flow through the mills and to the customer could be streamlined and optimised to ensure that defective or out of tolerance material is not sent through additional, expensive, value added processes[2,3]. The problem is that steel in the caster is at temperatures in excess of 800 °C and the environment is so harsh that most inspection technologies will not work under these conditions.

Engineering Doctorate Submission Number 2 contained a review of the literature whereby different inspection technologies were assessed and their suitability for inspecting the surface and internal quality of hot, moving steel were reviewed[4]. This review concluded that a non-contact ultrasonic technique should be selected, as this was suitable for the hostile environment and could find both internal and surface defects at the same time[4].

Engineering Doctorate Submission Number 3 was a further literature study that reviewed non-contact ultrasonics and showed that a Laser-EMAT (ElectroMagnetic Acoustic Transducer) system could be suitable for on-line inspection in the continuous casting plant[5].

Engineering Doctorate Submission Number 4 contained the results gathered after significant practical experimental research was conducted to find defects on hot, moving steel[6].

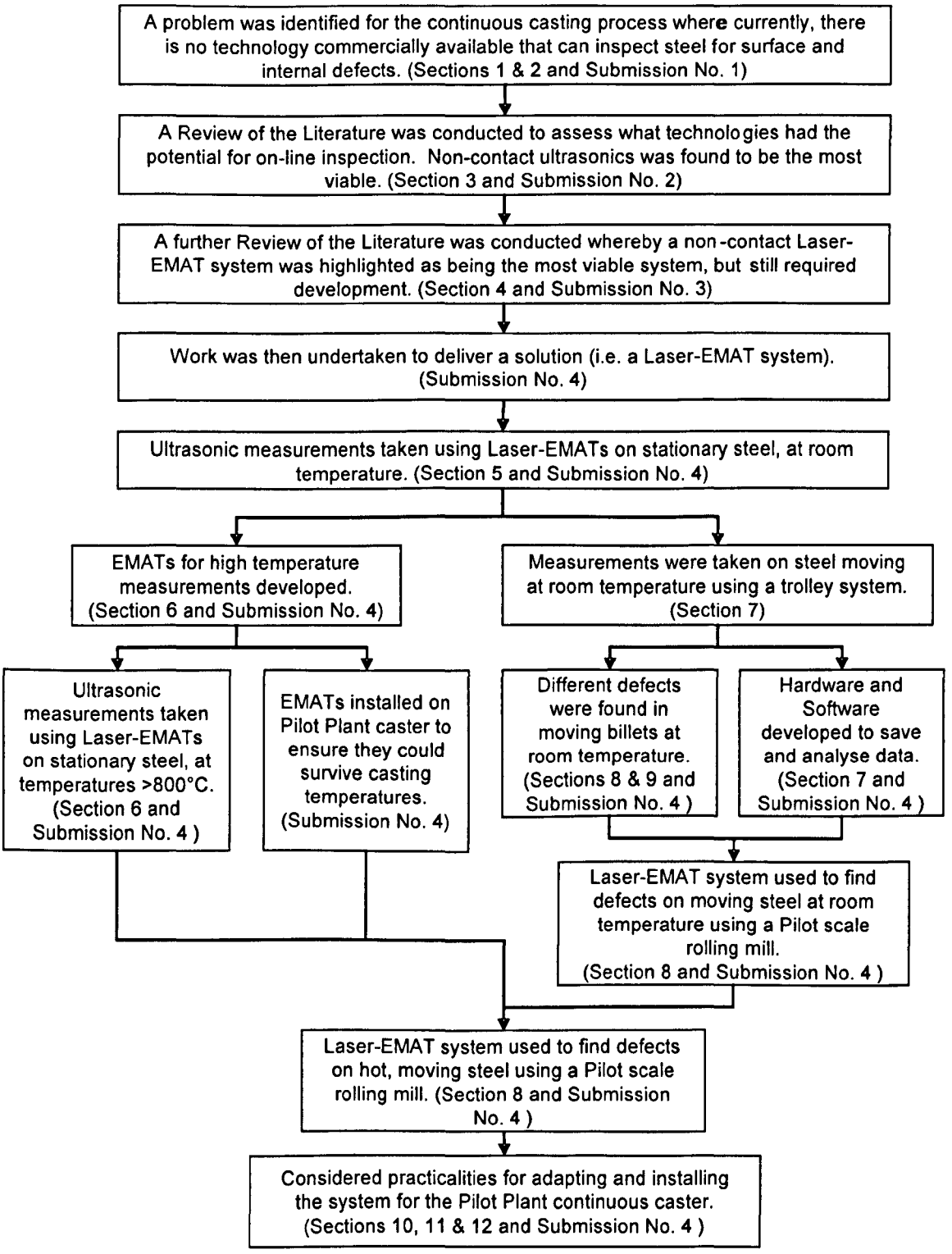

Fig. 1: Schematic diagram showing the main stages of the EngD project and how the individual portfolio submissions are linked into the sections of this Innovation Report.

2. THE CONTINUOUS CASTING PROCESS

During the complex continuous casting process, both surface and internal defects can arise in the as-cast semi steel products. This problem has been identified and there is a need to develop an automated, on-line inspection technique to examine the surface and internal quality of semis in the steel industry[1]. The harsh environment with surface temperatures in excess of 800 °C, water sprays and steam is not compatible with most measuring techniques. This was initially discussed in the first Engineering Doctorate submission entitled "An introduction to the defects caused during the continuous casting of steel and the need to detect them on-line"[1]. This showed that defects can be classified into two main categories - surface and internal. Surface defects include cracks, blowholes and inclusions, whilst internal defects can also include cracks, porosity, inclusions and segregation. Figure 2 shows an example of different surface and internal defects that can exist in continuously cast steel.

The industrial manufacturing process for first transforming liquid steel into rectangular solid steel products such as slabs, blooms and billets is typically via continuous casting machines which operate in a very harsh and hot environment[1,3,4]. These "as-cast" products are called 'semis' in the steel industry and are the precursors for the final rolled product.

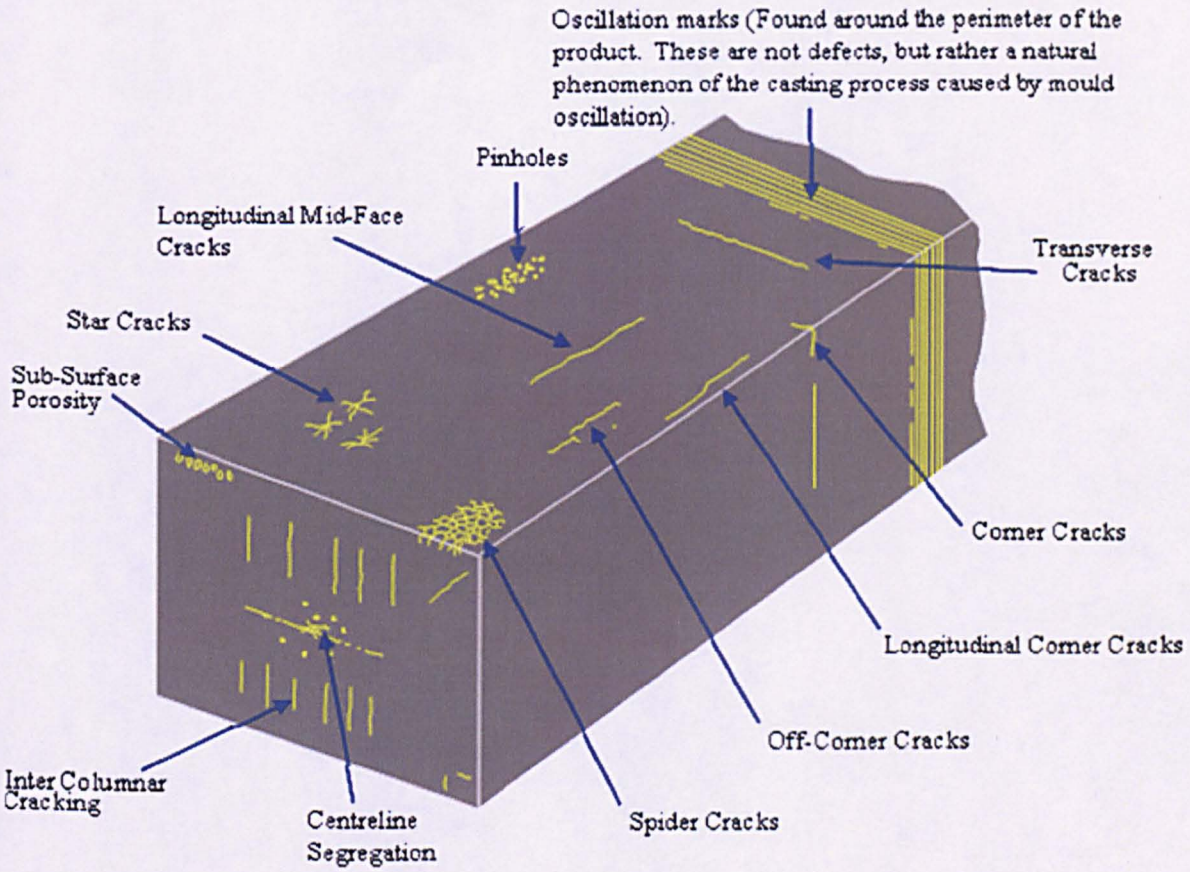

Fig. 2: A diagram showing various types of surface and internal defects that could be found in semis.

A diagrammatic view of a continuous caster can be seen in Fig. 3. This shows liquid steel being held in a refractory lined ladle, which may hold around 300 tonnes of liquid metal. When the ladle is positioned above the tundish, the steel flows through a ladle shroud (attached to the ladle to prevent oxidisation of the steel) and into the tundish.

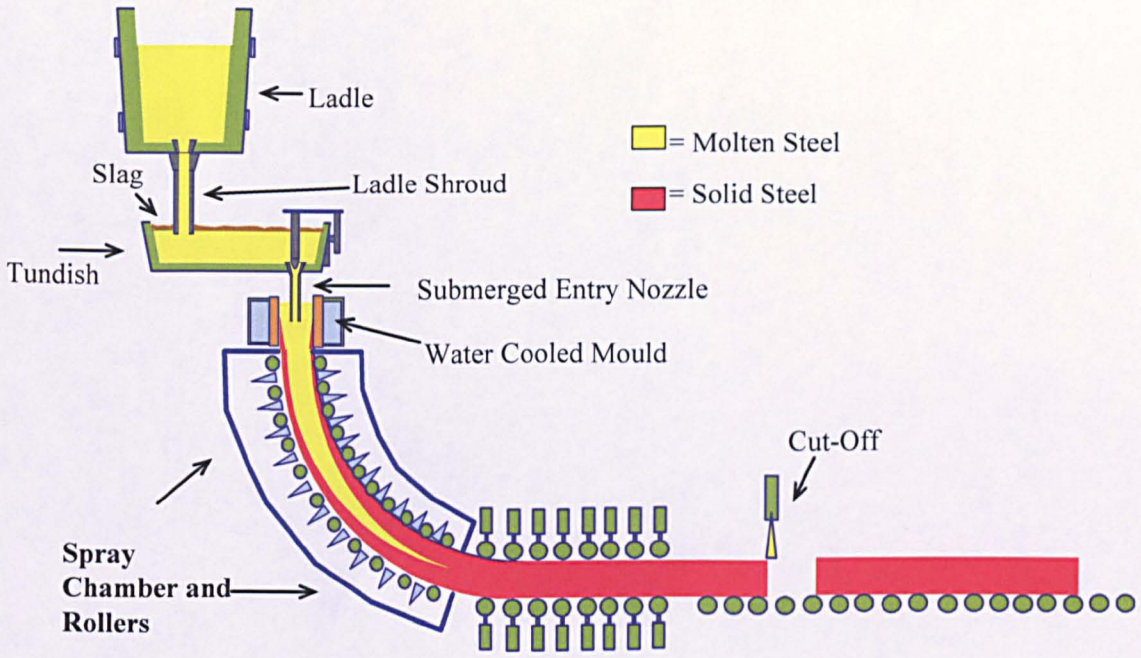

Fig. 3: A diagram of a continuous caster with key components highlighted.

The tundish is a smaller, refractory lined container that may typically hold around 30 tonnes of liquid steel which acts as a buffer between the ladle and mould and allows some inclusion floatation. The steel then flows through the tundish and out through the bottom via a Submerged Entry Nozzle (SEN) and into the mould. The mould is normally rectangular in shape and depending on the caster type, can be used to manufacture slabs, blooms or billets. The moulds are interchangeable, depending on the required product size. Rapid heat extraction occurs when the liquid steel first enters the water-cooled mould and this is necessary to form a solid outer shell to start the formation of the cast product. As the steel solidifies, it forms a long length of steel which is solid on the outside and molten on the inside and is called the "strand". The strand is then pulled down through the caster, using gravity and driven rolls. The strand is pulled through a water spray chamber and before the strand is cut into lengths of steel, it will have completely solidified through the entire thickness of the product. The strand is then cut to length to form semis, which can be up to 14 m long.

The continuous casting process is so named, because even whilst the strand is being cut to length at the cut-off point, new liquid steel is being constantly poured into the mould. When one ladle has been emptied, the tundish still holds a significant volume of molten steel and as the emptied ladle is removed, a new ladle is brought into position. This ladle will be opened and a fresh supply of liquid steel will be poured into the tundish, always keeping the tundish full until casting is ready to stop. Casting of several ladles is known as "sequence casting" and a sequence can last for several days.

The continuous casting process is extremely complex and different steel grades have different requirements when they are being cast. Manufacturing problems can arise that can affect the quality of the semis being manufactured, causing problems in downstream processes and for external customers. As can be seen from Fig. 3, a continuous caster comprises many complex parts, each of which need to operate in conjunction with one another and the operators to produce good quality steel.

3. THE IMPORTANCE OF ON-LINE INSPECTION TO REDUCING COSTS

The ability to inspect steel on-line would lead to significant process improvements and cost reductions in the steel manufacturing process. A letter of support, from the Technical Director of Corus Scunthorpe Works can be found in Appendix 1, which states some of the benefits an on-line inspection system could have to Corus. One of the major advantages for on-line inspection would be to alert operators to casting defects when the steel is being made, thereby giving them an opportunity to alter the casting machine to rectify the situation. Significant costs could be saved if defects were detectable earlier in the steel manufacturing process, rather than the defects causing problems for downstream processes or being contained in the final product which has been delivered to customers. The aim of on-line inspection is to correct and control the casting process to ensure that no defective or 'out-of-tolerance' material is supplied to internal Corus Business Units or external customers[1,2,7,8].

After casting, each semi is issued with a 'Quality Number'[9]. This Quality Number allows for certain quality tolerances to be permitted in the semi. For semis containing defects not permissible for one particular Quality Number, the steel would be rejected and then either scrapped or used for other applications, which is dependent on the steel grade. Therefore, knowing the size and type of defects per cast would determine whether the customer requirements were being met for that particular cast product.

3.1 Correcting Defects via Feedback Control during the Manufacturing Process

Having an automated, on-line inspection system could alert operators who could then alter casting parameters in near real time, should defects be detected. Therefore, rather than continuously cast several thousand tonnes of steel and manufacture semis that could potentially contain defects, defective material would be detected after a few minutes of casting, when the steel moves past an automated, fixed inspection point. Operators could then take steps to adjust casting parameters or stop casting entirely. This would lead to significant cost savings, as operators would be able to alter casting parameters whilst the steel was being made. Take, for example, a case of corner cracking which normally arises if there is a problem with spray cooling. If it is known that a semi contains this type of defect, then the operators can check and make adjustments to the casting machine, thereby correcting the source of the problem[3]. As semis can be tracked through the steel mill, any semis that contain defects could be closely monitored to ensure they do not cause problems downstream and routed accordingly.

3.2 Reducing the Amount of Manual Inspection and Delays in the Slab Yard

Only a small fraction of steel semis are ever manually inspected, due to the time taken to complete the assessment and the costs involved.

For surface inspection, normal practice is to inspect only quality critical steel grades after the semis have been cut and laid out in the stockyard. This only happens after a few days by which time the steel has cooled sufficiently to enable an operator to come into close proximity in order to conduct a manual, visual inspection or dye penetrative testing of the steel[4,10]. Looking for defects in this manner is very difficult because the surface is covered by oscillation marks

and iron oxide scale, making small defects very difficult to see. An on-line inspection system would inspect all semis for their surface quality, thereby allowing operators to send the semis to the relevant downstream processes without incurring significant delays.

For internal inspection, a thin slice is cut off the as-cast semi and the sample is prepared before taking sulphur prints for inspection. (Sulphur prints are taken using photographic bromide paper, soaked in sulphuric acid and pressed onto a ground steel surface. The sulphur print shows sulphur segregation which can outline the primary grain structure and internal defects.) Small representative samples may also be taken for metallurgical examination, using microscopes. This technique can only be completed after a few days when the steel has been cooled sufficiently and only checks a small volume of steel being cast. An on-line inspection system would be able to find internal defects throughout an entire semi, not just a small sample. With enough confidence in the system, the costly procedure involved in taking sulphur prints could be considerably reduced when replaced with an on-line system. This would reduce significantly the delays for downstream processes that currently need to wait for the sulphur print results before performing subsequent processing.

3.3 Reducing the Costs Associated with Scarfing

When a steel grade is required to have a very good surface quality, scarfing is conducted, which is a process whereby approximately 5 to 10 millimetres of the steel surface of a semi are removed using oxygen-propane torches that burn off the top, bottom and side faces of a slab. This means that only surface defects are removed provided they are shallower than the depth being scarfed off. This surface rectification is a costly process in terms of equipment, manpower and energy that can result in significant yield losses of up to 7%[4].

Scarfing, for some steel grades, is carried out as a "matter of course" i.e. whether the semis have any visible defects to the naked eye or not. Scarfing usually takes place after the slabs have cooled. After scarfing, the surface of the semis is assumed to be defect free. This assumption is made because only a handful of steel grades are ever inspected, again after scarfing due to time and manpower costs involved with manual inspection. It has been shown that even when slabs have been scarfed, they may still contain deep surface cracking[10], but these defects are often not found until the final product has been made. Being able to inspect slabs before they are scarfed would mean that only steel with surface defects that were shallow enough to be removed during the scarfing process would actually be scarfed. If deep defects are found, then more scarfing could be performed meaning the defects were completely removed. An inspection technique that could be used to gauge defect depth would therefore be advantageous. Any slabs with no, or minor defects, could by-pass the scarfing process thereby saving yield losses and costs.

4. HOW NON-CONTACT LASER-EMAT (ULTRASONIC) TECHNOLOGY WAS SELECTED BY REVIEWING THE LITERATURE

A variety of different on-line systems for both surface and internal inspection are available for use within the steel industry and these were assessed as part of a review of the literature[4], but some of the techniques cannot be applied in the manufacturing environment of the continuous caster. These harsh environments pose significant problems and therefore demand industrially robust sensors and instruments to accommodate this, for a variety of reasons, which include:

1) Large vibrations of the manufacturing machinery.
2) The hot, dirty environment caused by mould powder and iron oxide scale that can clog instruments and mechanical parts.
3) The temperature of the steel product can be in the range of 600 °C to 1100 °C and therefore there is a need to ensure that a sensor is not affected by the Curie Point which is approximately 770 °C.
4) Steel can be moving at speeds between 0.5 m/min and 5 m/min.

It is therefore highly desirable that sensors and instruments used in the steel industry be non-contact and are able to work at high temperatures so they can function reliably for an extended period of time in a harsh industrial environment with minimal maintenance requirements. This is because any sensor in physical contact with a casting strand would not survive for long unless it had excellent heat resistant properties. There is also a need to make any results from an inspection system suitably easy to interpret for operators or for an automated inspection system.

A summary of different inspection techniques available is given in Table 1, along with an assessment of their suitability for on-line inspection in the unique operating environment of the steel industry. Each of these technologies is considered in Engineering Doctorate Submission Number 2[4]. From Table 1, it can be seen that the only technique available for inspecting the internal quality of a "semi" on-line is ultrasonic. Surface quality could be assessed using ultrasonics or alternative methods such as Eddy current[11-14] and Conoscopic Holography[10,15-17]. However having a system that could find internal and surface defects at the same time should be the most cost effective. Because the steel is moving and is in excess of 700 °C, any contact ultrasonic method can be eliminated from the list of potential systems as any probe or sensor within such close contact with the hot, moving steel would not survive for long due to the harsh environment and therefore a non-contact ultrasonic system must be used.

The literature was investigated further to ascertain what the current non-contact ultrasonic state-of-the-art system could be and to investigate the possibility of using such a system in the steel industry[5]. This Engineering Doctorate Submission detailed some of the work accomplished by some of the major worldwide steel manufacturers, universities and companies working in the non-contact ultrasonics field at high temperatures and showed that no system was commercially available off-the-shelf.

Ultrasound can be generated in steel by several non-contact methods[4-6]. According to the Review of the Literature conducted as part of this project, the method most likely to generate a sufficient amount of ultrasound to make internal inspection possible in steel is through the use

of a high energy, pulsed laser beam system[4-6,18-28]. Reception of the ultrasound can be via an electromagnetic coupled device such as an EMAT (ElectroMagnetic Acoustic Transducer) or a laser interferometer system[4-6,29-31]. Ultrasonics can also be used to gauge crack depth[11].

Laser interferometers are prohibitively expensive and multiple interferometers would need to be purchased to inspect a steel slab. However, relatively inexpensive EMATs could be used in an array configuration to detect defects. From the review of the literature[4,5], it could be shown that Laser-EMAT technology had the potential for being engineered for the high temperature, on-line inspection of semis[4,5,21,29,32-36]. Laser-EMAT systems have been developed in the past for on-line inspection of steel plates at room temperature and hot pipes, although neither of these systems is available commercially [37-40].

Table 1

Summary of different inspection types, indicating the suitability of each technique for inspecting hot, moving steel

	Can technique be used on-line?	Is the technique non-contact?	Can it be used at temperatures > 700°C?	Suitable for surface, sub-surface or internal defect detection?	What are the disadvantages of the technique?
OPTICAL TECHNIQUES					
Human Visual Inspection	Y	Y	Partially	Surface only	Open to human interpretation
CCD/Video Camera	Y	Y	Y	Surface only	Scale/rough steel surface gives false readings
Conoscopic Holography	Y	Y	Y	Surface only	Only for use on longitudinal cracks
Laser Triangulation	Y	Y	Y	Surface and sub-surface*	Large defects only
Scarfing Spark	Y	Y	Y	Surface and sub-surface*	Automated system not as quick as manual scarfing
THERMAL TECHNIQUES					
Infrared Camera	Y	Y	Y	Surface only	Scale/rough steel surface gives false readings
ELECTROMAGNETIC TECHNIQUES					
Eddy Current	Y	Y	Y	Surface and sub-surface*	Surface. Sub-surface possible if steel is above Curie Point.
ULTRASONIC TECHNIQUES					
Piezoelectric	Y	N	N	All	Contact and needs couplant
ElectroMagnetic Acoustic Transducers (EMATs)	Y	Y	Y	Surface and sub-surface*	Small stand-off. Difficult to probe for internal defects when hot.
Laser-EMAT	Y	Y	Y	All	Small stand-off for EMAT
Laser-Laser	Y	Y	Y	All	Expensive. Sensitive to surface finish, e.g. scale
Sperry Wheel	Y	N	N	All	Contact. Corus system does not work on products >1cm
OTHER TECHNIQUES					
Dye Penetrant	N	N	N	Surface only	Off-line
Sulphur Printing	N	N	N	Internal only	Off-line. Only small sample taken from steel cast
Magnetic Flux Leakage	Y	Y	N	Surface only	Only useful for steel below Curie Point
Magnetic Particle Inspection (MPI)	Y	Y	N	Surface only	Lack of automatic focusing and needs a flat surface
X-Rays and Gamma Rays	N	Y	N	Surface only	Cannot be used on moving objects
Microwave	Y	Y	Y	All	Large defects only

* = Subsurface is approximately within 10mm depth.

5. STEPS TAKEN TO DEVELOP AN ON-LINE SYSTEM

The review of the literature showed there was no commercially available Laser-EMAT system suitable for on-line inspection of hot, moving steel[3]. Therefore research and development work was undertaken to develop technology that was laboratory based and primarily designed for testing stationary cold steel (i.e. steel at room temperature) in order to create a novel, prototype system suitable for the on-line inspection of hot (i.e. steel above 600 °C), moving steel. At the start of the Engineering Doctorate, the expertise rested with the Ultrasonics Group at The University of Warwick, who could test stationary steel samples at room temperature and find defects in the steel. Some high temperature trials have previously been conducted at Warwick in the mid 1990s and the results of these have been published[19,20]. At Corus, expertise was developed and a new facility where Laser-EMAT technology could be designed and developed in order to inspect moving steel at high temperatures was built as part of this project.

Corus has pilot scale mills at its two UK research sites; Teesside and Rotherham. The facilities used as part of this project are summarised in Table 2. Standard practice at Corus involves rigorously testing any new equipment on the pilot mills before installing it in a commercial manufacturing plant. Therefore, Corus utilises pilot plants (i.e. smaller versions of the manufacturing machinery steel plants) to conduct a series of tests under different controlled conditions to validate systems. The following sections demonstrate how these facilities were used to validate the Laser-EMAT system.

Table 2

A list of facilities used during the course of the project

Location	Facility Name	Description
Teesside (TTC)	Vertical Continuous Caster	• 3.5ton caster, capable of producing 7m lengths of billets • (Decomissioned in 2004)
Teesside (TTC)	Horizontal Continuous Caster	• 7 ton caster, capable of producing 70m lengths of billets • (Comissioned in 2006)
Teesside (TTC)	Roller Straightner Mill	• Can move billets using driven rolls
Teesside (TTC)	Laboratory	• Constructed for sole use in EngD project - Automated trolley system for moving steel samples - Kilns constructed to heat metal samples • Contains 800mJ, fixed position laser system
Rotherham (STC)	Rolling Mill	• Can move billets using driven rolls. • Can roll billets • Automatic Descaler • Furnace heats billet (Max length 1m)
Warwick	Ultrasonics Laboratory	• Contains a furnace for heating steel samples • Contains 1064nm & 532nm Nd:YAG and CO_2 pulsed lasers

6. LASER-EMAT THEORY

6.1 The Laser Beam as a Broadband Ultrasonic Source

Defects in steel can be detected (i.e. their location found and sized) using ultrasonics. In Laser-EMAT technology, a pulsed laser beam incident on the sample surface can generate ultrasonic waves in steel[18-28]. This happens when a high energy density pulsed laser beam (at Corus this is 800 mJ at 1064 nm with a beam diameter of 6 mm or a different laser with 150 mJ at 532 nm with a beam diameter of 5 mm) is incident on a sample surface, resulting in a plasma being formed from ablation of the steel surface and breakdown of air[21]. At room temperature, approximately 4% of this energy is absorbed by a clean steel surface and some of this energy is converted to ultrasound[21]. The shape of the impact point on the steel is approximately circular, as this represents the natural shape of the laser beam. The diameter of the impact point is dependent upon the focused laser beam diameter and when this is significantly less than the ultrasonic wavelength considered, then the laser beam can be considered as a point source. (The optimal laser beam diameter was determined by experiment[6] by acquiring ultrasonic waveforms at different focal lengths for a particular EMAT design). When viewed from above, a laser beam point source will generate surface wavefronts that are approximately circular on the surface of the sample and these can be seen in Fig. 3a. A point source will generate wavefronts on the surface of the sample that are surface waves which are 2-D in nature and can be seen in Fig. 3b. The use of bulk waves to find internal defects is detailed in Section 6.4.

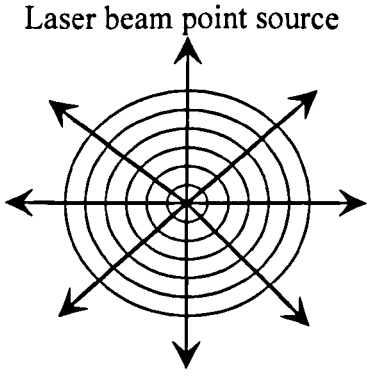

Fig. 3a: Plan view of wavefronts emanating from a point source.

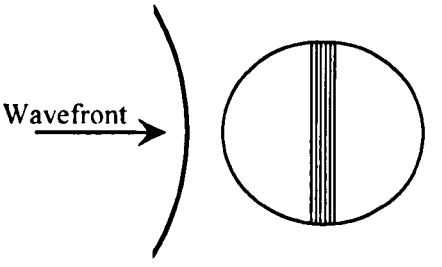

Fig. 3b: Plan view showing the curved wavefront reaching the linearly wound EMAT coil.

6.2 The EMAT as an Ultrasonic Receiver

An EMAT can be used to detect ultrasonic signals. An EMAT operating predominantly via the Lorentz mechanism, was used in this project. This EMAT is essentially a static magnetic field with a plane of a coil of wire, where the direction of the wires of the coil are perpendicular to the static magnetic field[29-31].

The approach to monitoring the received ultrasonic signals is dependent upon the alignment between the linear EMAT coil and the crack orientation. Therefore the relative position and distances between the EMAT coil, laser and defect are all-important. This configuration is also dependent upon the dimensions of the steel product.

6.3 How Surface waves can be used to Find Defects

On thick samples where the wavelength of ultrasonic waves generated by the pulsed laser beam is very much less than the thickness of the steel, both Rayleigh surface waves and bulk waves can be generated simultaneously by the broadband laser ultrasonic source. The surface waves observed are surface skimming compression (P-waves) and Rayleigh (R-waves). The path of the direct R-wave, between the laser and EMAT can be seen in Fig. 4a. This is the same path taken by the P-wave. Rayleigh waves can also be reflected off the sides of the steel, and these reflected waves can be seen in Fig. 4b. R-waves can also be reflected off defects. These R-waves and P-waves can be used to locate and size defects.

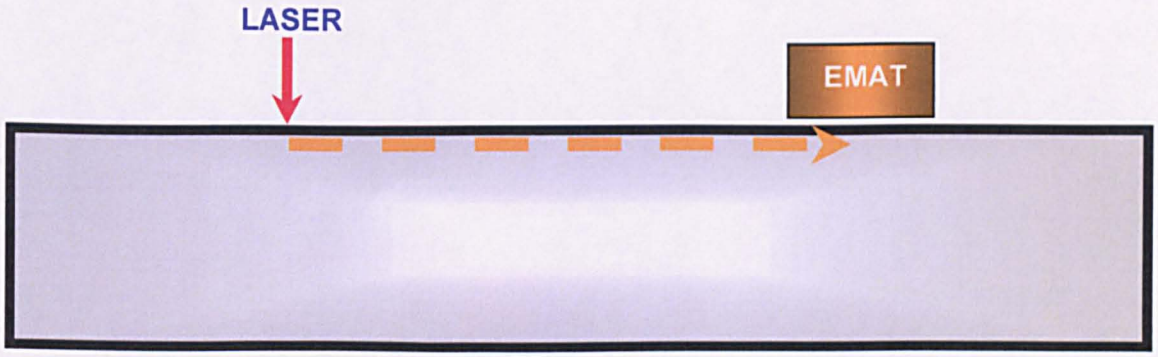

Fig. 4a: Path of the direct R-wave and P-wave.

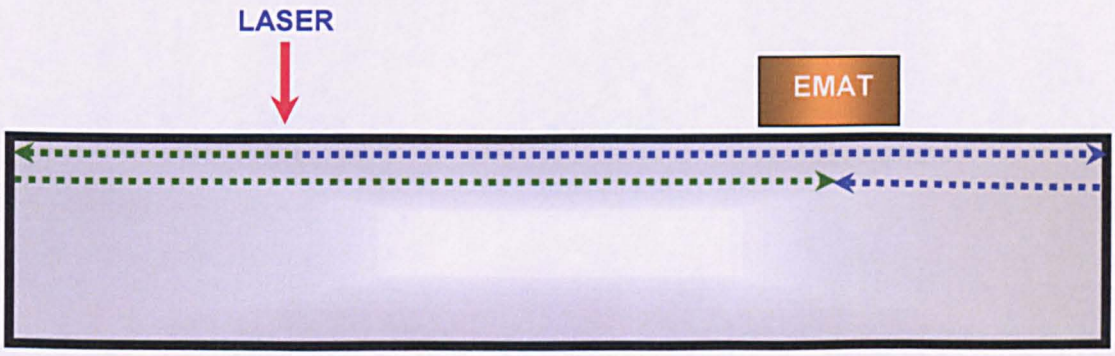

Fig. 4b: Path of the R-waves being reflected from either side of the sample.

The system is optimally sensitive when the linear EMAT coil is approximately parallel to the defect as shown schematically in Fig. 5a. If the defect is perpendicular to the coil, then it is not so easily distinguishable directly, as shown schematically in Fig. 5b, but can often be detected via reflected waves, as shown schematically in Fig. 5c. Coils should therefore be oriented towards the regions where defects exist. On semis, surface defects are typically on the edges of the product, or in the middle face. These defects are mostly either transverse or longitudinal and therefore coils should be favourably oriented to find these types of defects. A description of an EMAT array, whereby both transverse and longitudinal defects could be found can be seen in Section 11.

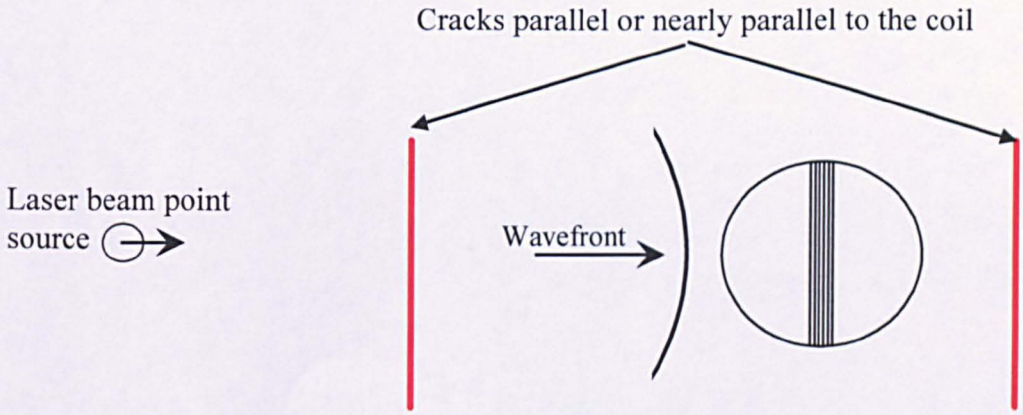

Fig. 5a: Plan view of wavefronts emanating from laser, where the cracks are parallel, or nearly parallel to the wavefronts. The EMAT coil should easily detect these signals.

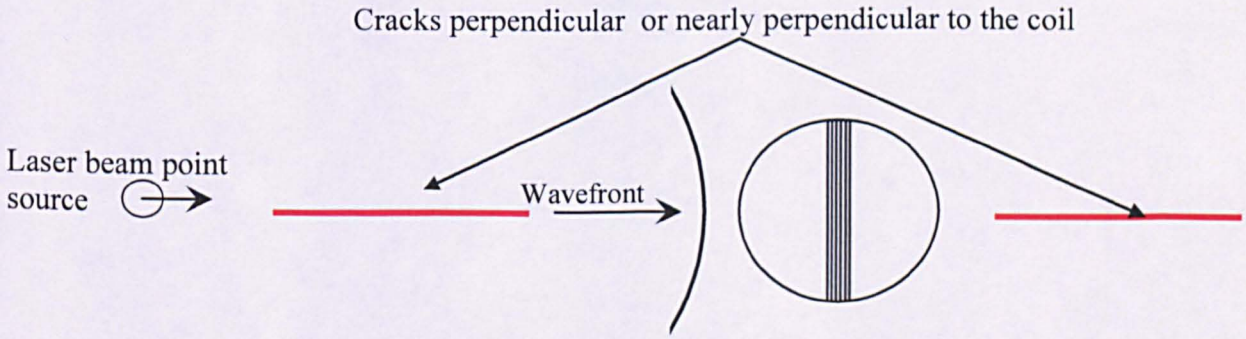

Fig. 5b: Plan view of wavefronts emanating from laser, where the cracks are perpendicular, or nearly perpendicular to the wavefronts. The EMAT coil may not easily detect these signals.

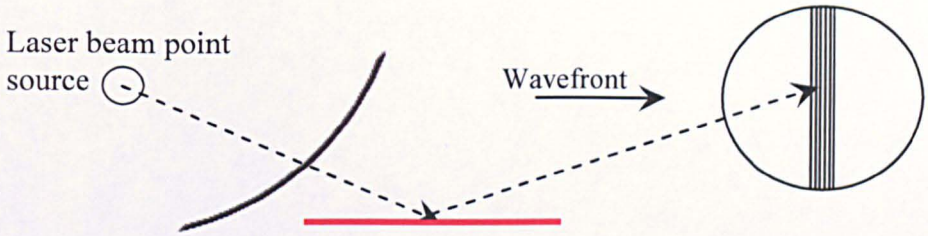

Fig. 5c: Here, a wavefront is being reflected off the crack and detected by the EMAT.

Figure 6a shows a plan view of a steel sample, showing the relative position of a laser beam and EMAT coil. Here, the direct R-wave is indicated on the schematic and the arrival time of this wave can be calculated using the equation $t = d/v$, where t is time, d is distance between laser beam and EMAT coil and v is the velocity. The arrival time of the Rayleigh wave can then be calculated using the velocity of ultrasound in mild steel at room temperature (2996 ms^{-1}[41]) provided the distance between the laser generator and EMAT receiver is known. The P-wave travels the same distance, but has a velocity of 5960 m/s[41] and therefore this wave arrives at approximately half the time of the direct R-wave. An accurate method for determining the velocity of ultrasound in steel is detailed in Engineering Doctorate Submission Number 4[6].

The R-wave is clearly distinguishable as it has significantly higher amplitude as compared with the P-wave and indeed the other ultrasonic waves. This is mainly due to the R-wave having a lower geometric attenuation. The R-wave can also be reflected from the edges of a sample and be detected by the EMAT coil.

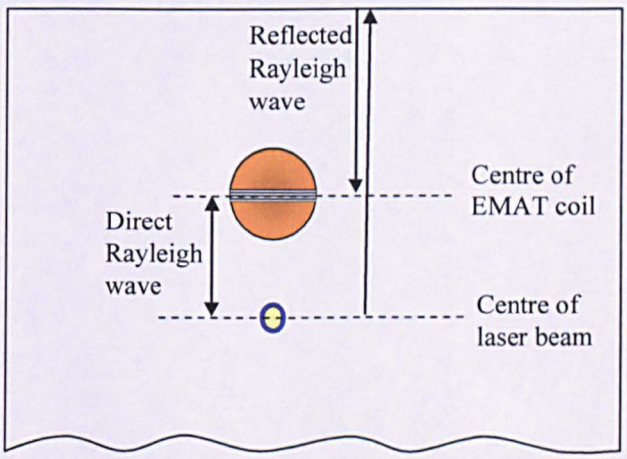

Fig. 6a: Plan view of the billet being tested. Nothing is blocking the path between the laser and EMAT.

Figure 6b shows a plan view of a steel sample, showing a defect blocking the direct path between the laser beam and EMAT coil. Because the Rayleigh wave is broadband, lower frequency components of the Rayleigh wave with wavelengths longer than the defect depth can at least partially propagate under a defect and be detected by the EMAT coil[18]. The R-wave that propagates under the defect may also have enough energy to be reflected off the sample edge and still be detectable by the EMAT. However, for deep defects typically greater than the

wavelength, the R-wave can be attenuated so much that it is not detectable[18]. The P-wave might also be detectable some distance after the crack, but may not be detectable immediately after the crack. It can be detected if the EMAT is located further away from the defect as the P-wave is associated with a bulk compression wave. The R-wave can also take longer to arrive when a defect is present due to only the lower frequency content passing under the defect and it requires some propagation distance fro the crack for energy to propagate back up to the surface boundary.

A detailed example of how a defect can be found when the steel is moving is given in Section 9.

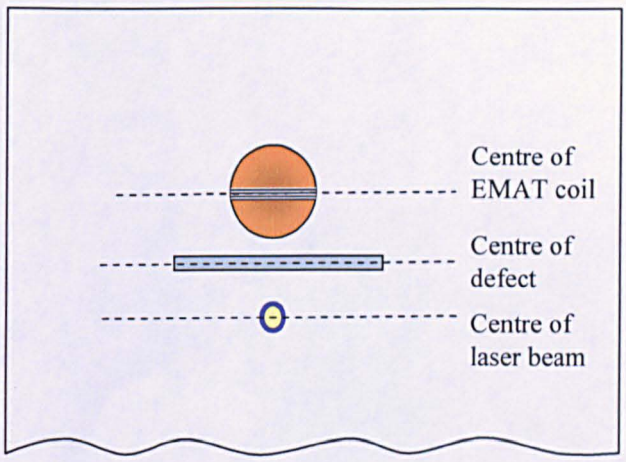

Fig. 6b: Plan view of the billet being tested. Here, a defect is blocking the path between the laser and EMAT.

6.4 How Bulk Waves Can be Used to Find Internal Defects

When the laser beam and EMAT are positioned on the top surface of the steel, in addition to the R-wave, shear (S-wave) and longitudinal (L-wave) waves can both be generated simultaneously. The attenuation of bulk and Rayleigh waves is different, due to the way their energies are spread. The energy of the R-wave is localised on the surface around a circumference of a circle, whereas bulk wave energy is localised on the surface of a hemisphere and is therefore geometrically attenuated more strongly than the R-wave. The exact distribution of bulk wave energy is non-trivial[21]. These bulk waves reflect off the bottom surface of the sample and can then form shear bulk waves (SS) and longitudinal bulk waves (LL). This path can be seen in Fig. 7a. Additional waves can also be detected, such as SL (shear to longitudinal waves) and LS (longitudinal to shear waves) which have mode converted on reflection from the back surface and the path of these waves can be seen in Fig. 7b. In addition to these waves, multiple wave reflections can occur, and these include the following wave combinations; LLLL, LLLS, LLSL, LSLL, SLLL, LLSS, LSLS, SLSL, SSLL, LSSL, LSSS, SLSS, SSLS, SSSL and SSSS. Typically, the largest detectable waves from the listed combinations involve those with the least number of mode conversions, i.e. the LLLL and SSSS, followed by the LLLS and SLLL waves. However, it should be noted that the appearance of these waves is dependent on a number of factors including; the characteristics of the generation source used, the characteristics of the receiver, the dimensions of the steel and the distance between the generator and receiver. Bulk waves can also be reflected off the side and bottom sample faces. These waves can comprise the following combinations; SSS, SSL,

SLS, LSS, SLL, LLS and LLL. Again, the largest detectable waves from the listed combinations typically involve those with the least number of mode conversions, i.e. the LLL and SSS, followed by the LLS and SLL waves. Reflections and mode conversions of L-waves and R-waves also occur from the side walls of the steel under test. These bulk waves can be used to find internal defects.

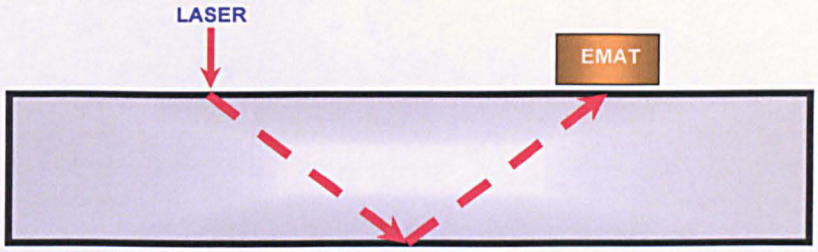

Fig. 7a: Path of the LL and SS waves.

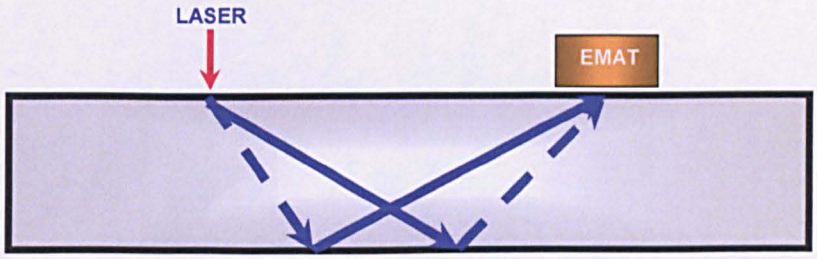

Fig. 7b: Path of the LS and SL waves. The dotted line represents the path of the S-wave and the solid line represents the path of the L-wave.

6.5 Optimising a Laser-EMAT System

It should be noted that a fully optimised Laser-EMAT system is dependent on a variety of different factors which include:

- The type of pulsed laser system being used (e.g. the wavelength of the laser, pulse width, energy output, laser beam diameter etc.).
- The type of EMAT coil used and the dimensions of the coil (e.g. number of coil turns, diameter of coil used, overall coil width, magnetic field strength etc).
- The type of EMAT pre-amplifier used (the amplifier will contain electrical components which will be tuned to the frequency of the ultrasonic waves).
- The type of hardware filter used to remove extraneous noise from the ultrasonic waveform.
- The surface and material characteristics of the sample being tested. For example, different surfaces will vary the frequency dependant attenuation. Scale may also affect the performance of both the laser generation source and the EMAT and the presence of scale is discussed later in Section 7.1.

Therefore a balance was achieved via experimentation whereby all these different factors were weighed and considered so that the best possible quality data can be recorded, as detailed in the previous submission[6].

7. DEVELOPMENT OF AN EMAT SENSOR CAPABLE OF WITHSTANDING TEMPERATURES GREATER THAN 1000 °C

7.1 Mechanisms that Affect Ultrasonic Signals when the Steel is Hot

Different factors affect the measured amplitude of the ultrasonic waveforms at high temperatures. The EMAT used in these particular experiments utilises both the Lorentz force and magnetoelastic mechanisms when the steel is ferromagnetic (i.e. below the Curie point which is approximately 770 °C). At room temperatures, below the Curie point, ultrasonic attenuation is relatively lower and consequently the waveform amplitudes are typically very high and a good signal to noise signal ratio can be achieved.

When the temperature is above the Curie point, the following effects are evident:

- The amplitude of the ultrasonic waves detected by the EMAT decrease due to the changes in the material properties of the sample. There is an increase in the attenuation of the received ultrasonic signals. This means the signal amplitude is decreases. Above the Curie point, when the steel is paramagnetic, the magnetoelastic mechanism is lost and electrical conductivity decreases and therefore the EMAT becomes far less sensitive to ultrasound[19].
- One advantage, according to Scruby[21], is that 35% less optical power from a laser is needed to generate the same amount of ultrasound at 1000 °C than at 0 °C. More energy is absorbed by the hot steel at higher temperatures. The skin effect of the steel also varies with temperature. The skin effect is important as it affects the absorption of the laser energy and therefore the resulting size of the ultrasonic waves generated in the steel. This is in contrast to the point raised above.
- The magnetic field generated by the NdFeB magnet used in the EMAT decreases with temperature because the magnet temperature increases, meaning there is a drop in the magnetic field strength. This means the received signals have a smaller amplitude.
- The average grain size increases as the steel is heated. Larger crystals cause the ultrasound to attenuate further[42].

The amplitude of received ultrasonic waves is also dependent on the formation of scale/oxide on the surface of the steel[19,34]. If the scale is very well adhered onto the surface, the ultrasonic signals can increase in amplitude when the magnetite scale (Fe_3O_4) is below its Curie point at approximately 550 °C. Any loose, flaky scale needs to be removed, as the ultrasound cannot be detected efficiently due to the poor coupling between the steel and the scale. This problem could potentially be overcome by using wire brushes, compressed air or an electromagnet, which could be used to remove loose scale prior to the steel passing the EMAT sensors in a production plant. Scale was not problematic during the hot trials conducted as part of this project[6].

In order to overcome some of the problems evident when using EMATs at high temperature, the EMATs used in this project were designed to have the largest stand-off (i.e. distance) between the EMAT and the hot steel. This was to try and heat protect the EMAT, yet still allow for signals with a good signal-to-noise ratio to be received. Typically, the further away the EMAT is from steel, the smaller the signal-to-noise ratio becomes. In order to accomplish

this, rare earth NdFeB magnets (which were bonded and sintered) were used as these had a large magnetic flux density, measuring 460 mT at the surface of the magnet.

In order to protect the thin coil of the EMAT from damage, the magnets were first wound with a length of 3 mm wide double-sided tape. The coil was then wound parallel to the tape edge, to ensure it was wound as tightly together as possible. Using the tape, the enamel from the copper wire was not damaged when it was bent around the 'sharp' corners of the magnet. A schematic diagram of how the tape and coil was linearly wound can be seen in Fig. 8.

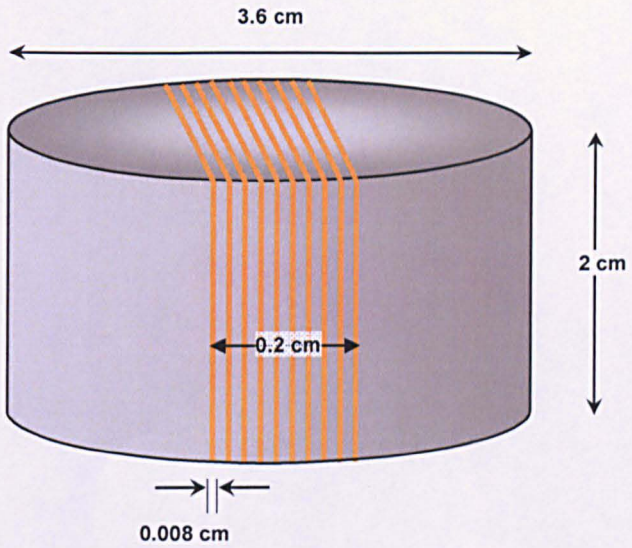

Fig. 8: A schematic of a NdFeB magnet, wound with thin enamelled copper wire to form an EMAT sensor.

From manufacturer's data[43], the NdFeB magnet had a Curie temperature of 120 °C. When a permanent magnet exceeds its Curie temperature, it loses its magnetism, thereby making any EMAT sensor ineffective. The magnet can survive brief time intervals where the Curie point is exceeded, but this cannot be prolonged without incurring irreversible damage meaning the magnet is demagnetised. In order to solve the problem, a water-cooled EMAT was designed, built and successfully tested[6]. An 'exploded' view of the water-cooled EMAT can be seen in Fig. 9.

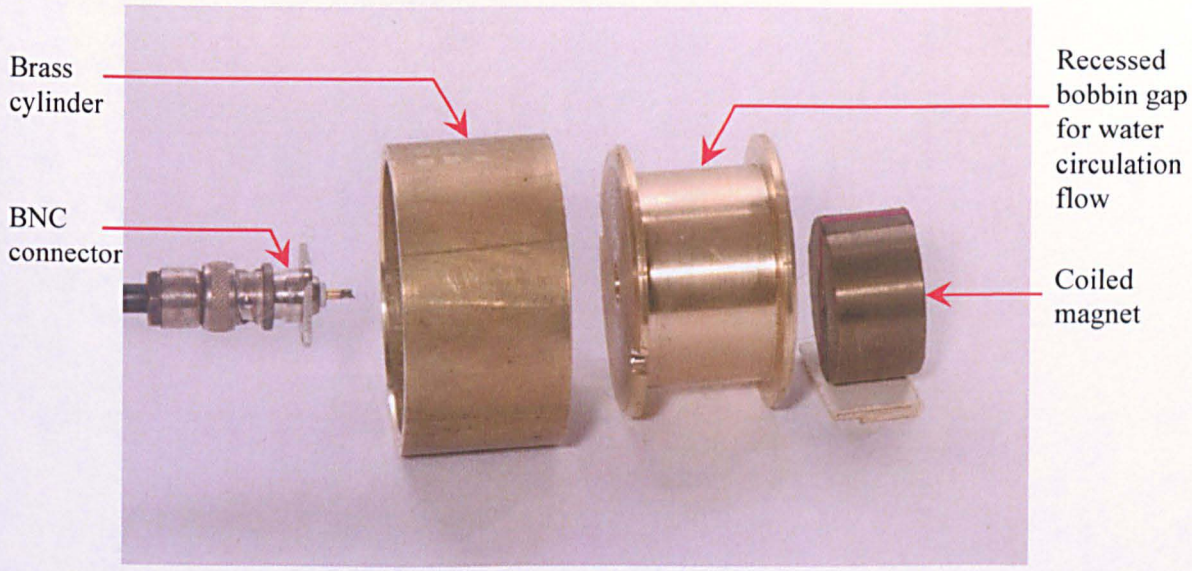

Fig. 9: Photograph of the EMAT 'exploded' to show the main parts.

The EMAT coil had to be protected from any damage by covering the coil with Kapton tape. A 0.5 mm thick alumina tile was then glued into a recess on the EMAT face to thermally protect the front face of the magnet and the EMAT coil. Because the thin coil was susceptible to damage, a thin sheet of austenitic stainless foil was used to cover the EMAT face. Stainless steel has a low electrical conductivity and a low magnetic permeability and therefore the cover did not significantly impair the function of the EMAT. The foil also helped to reflect heat from the hot steel. A schematic diagram showing the different layers used to protect the EMAT can be seen in Fig. 10.

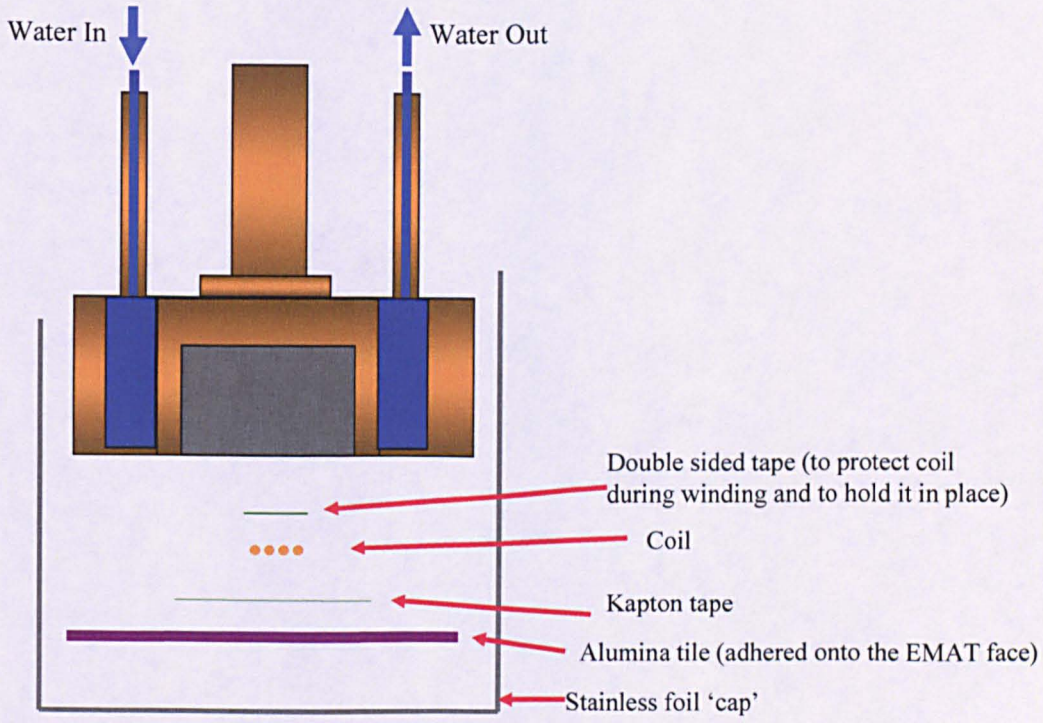

Fig. 10: Schematic showing the different layers used to protect the EMAT face (not to scale).

Figure 11 shows one of the completed water-cooled EMATs that was used in subsequent trials.

Fig. 11: The foil, folded and held in position with a jubilee clip.

7.2 Ultrasonic Experiments on Hot Steel Samples

An experiment was designed to test the performance of the water-cooled EMATs for the detection of ultrasonic signals at elevated temperatures at Teesside Technology Centre. In order to do this, a steel sample was positioned in a kiln on a scissor trolley, where the sample could be heated to over 1000 °C, as shown in Fig. 12. This allowed the sample to be heated up some distance away from the vertical firing laser system. After heating, the trolley was wheeled into position and its height adjusted inside the cabinet.

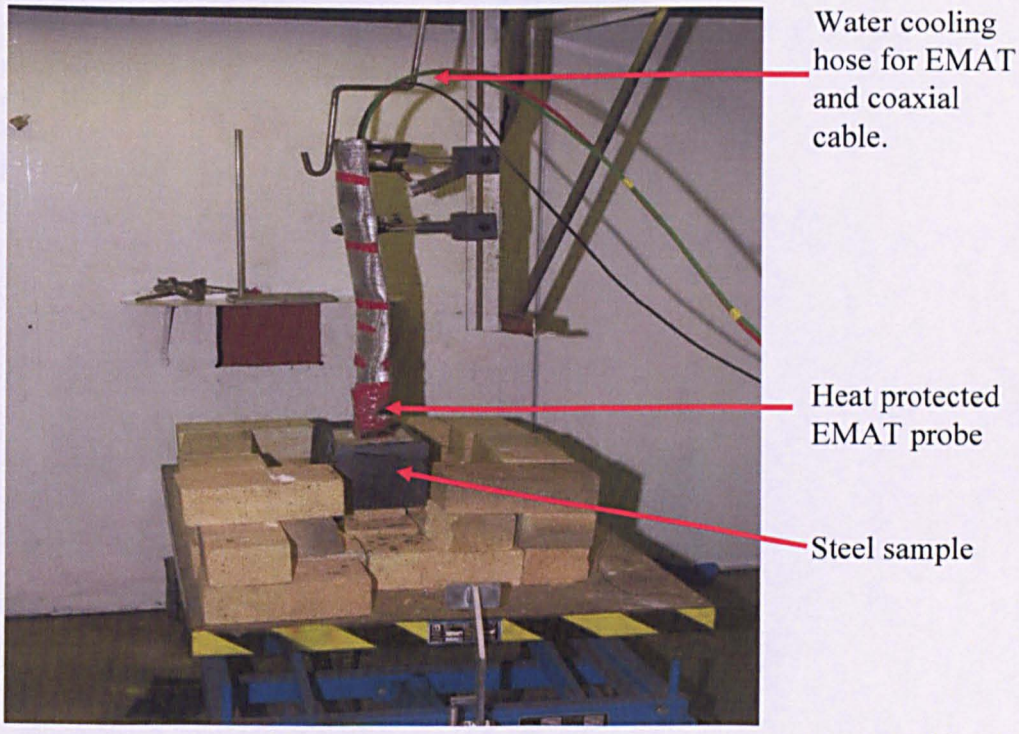

Fig. 12: A heated billet, positioned under the Laser-EMAT system.

Figure 13 shows a schematic diagram of the apparatus that was used in the initial experiments. Here, the laser beam was directed through a glass plate. Around 2% of the light is then reflected off this plate and onto a photodiode circuit wired up in reverse bias. When the photodiode receives the light from the pulsed laser beam, it produces a sharp positive voltage signal, which can be used as a trigger for the oscilloscope data logger. The majority of the laser beam energy passes through the glass plate and is then focused through a lens onto the surface of the steel, thereby generating the ultrasound. The water-cooled EMAT was placed on top of the steel surface. An amplifier and a filter were used to increase the signal to noise ratio of the signal received by the EMAT, filtering out background electrical noise with significantly different frequency content to that of the laser generated ultrasonic waves.

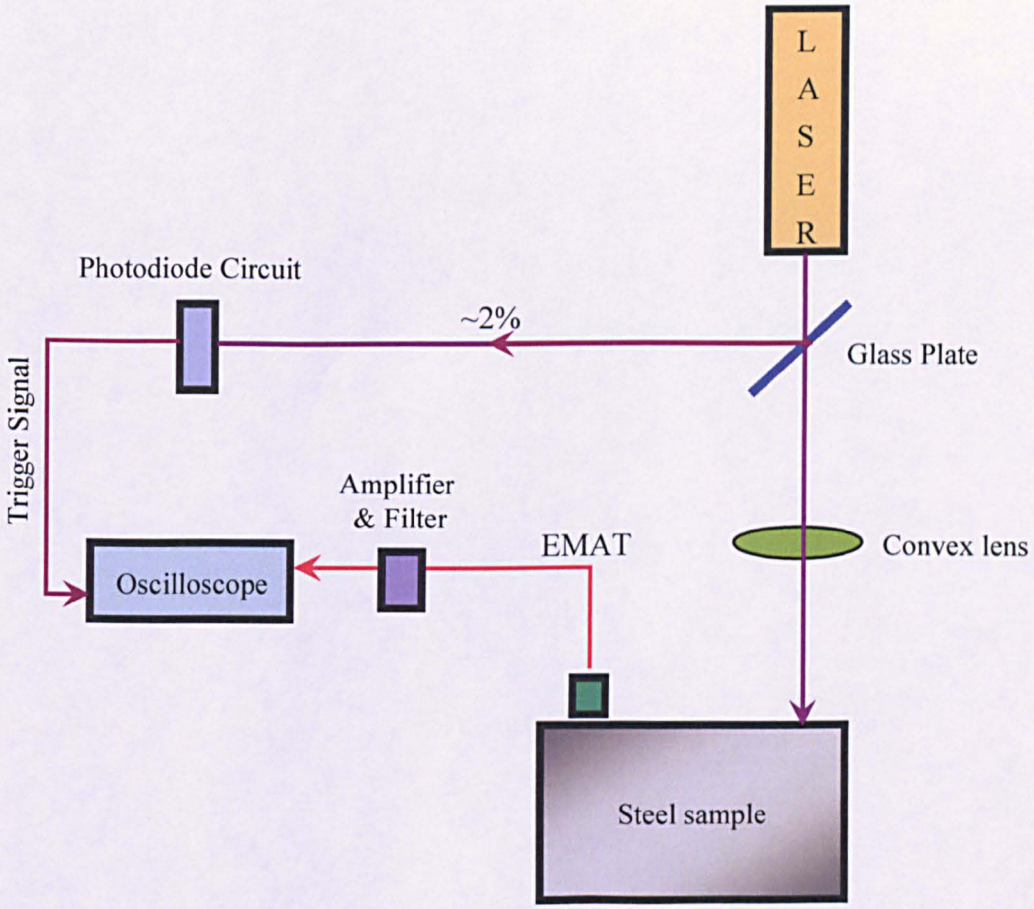

Fig. 13: Experimental Laser-EMAT arrangement.

7.2.1 ***Results***

Initially, it was thought that the formation of magnetic oxide scale could be problematic as the billet was heated and cooled. This was not the case in practice and no significant amount of magnetite "mill scale" was produced. The oxide scale that formed on the surface of the steel was very well adhered. A wire brush was used to try and dislodge any loose scale, but the scale was too well adhered. Because of the time taken to move and position the trolley in the correct position under the laser beam, the sample had cooled by a few hundred degrees Celsius. Therefore the first measurements were taken with a temperature of 840 °C $\pm$ 10 °C.

A thermocouple was used to measure the temperature of the sample surface and another thermocouple was inserted into a drilled hole in the centre of the sample to measure the internal temperature. The ultrasonic results from the hot billet over a range of temperatures can be seen in Fig. 14, showing that the ultrasonic signals' amplitudes are reduced significantly at higher temperatures. It can be seen from the graphs that as temperature rises, the velocity of the ultrasonic waves decrease leading to the observed increase in the arrival times in the various waveforms.

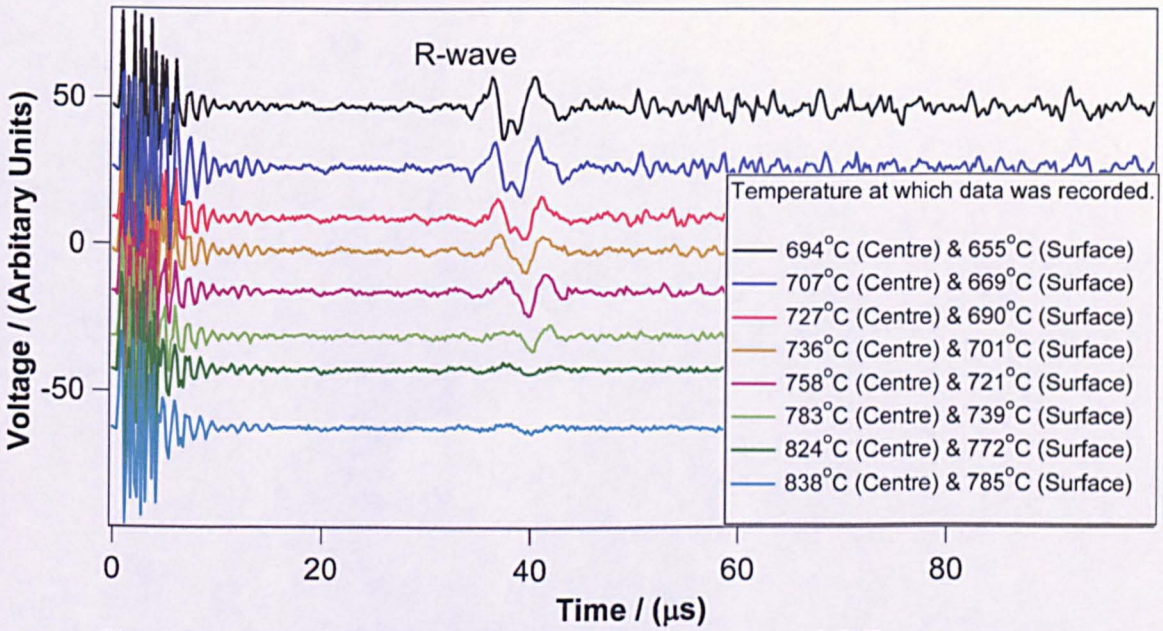

Fig. 14: Averaged ultrasonic signals taken at a variety of different temperatures.

The RMS (Root means squared) of the signal and noise was found before calculating the signal-to-noise (S/N) ratio for each of the A-Scans. The RMS was calculated by:

$$RMS = \sqrt{\frac{1}{n}\sum Y_i^2} \qquad \text{(Equation 7.1)}$$

Where n is the number of points and Y_i is the relative amplitude of the signal.

The standard deviation, (STDEV) is calculated by:

$$STDEV = \sqrt{\frac{\sum (y_i - \bar{y}_i)}{n-1}} \qquad \text{(Equation 7.2)}$$

The RMS noise value was taken at a point after the surface skimming P-wave and before the Rayleigh wave. This was because there was still noise from the laser pulse immediately before the P-Wave. The RMS of the signal was taken of just the R-Wave.

The following equation was used to find the S/N ratio:

$$S/N\ Ratio = 20.\log_{10}\frac{RMS_{Signal}}{RMS_{Noise}} \qquad \text{(Equation 7.3)}$$

A table of results can be seen in Table 3, which shows a general trend that as temperature increases, the S/N Ratio decreases. It should be noted that the RMS values approach the STDEV values.

Table 3

Table of S/N Ratios for A-Scans obtained at different temperatures

Temperature (°C)	694	707	727	736	758	783	824	838
RMS Signal (Arbitary Units)	5652	5253	4169	3463	3538	2036	991	970
STDEV Signal (Arbitary Units)	5698	5310	4220	3496	3563	2057	1004	980
RMS Noise (Arbitary Units)	871	797	756	777	704	559	535	437
STDEV Noise (Arbitary Units)	738	688	650	651	589	554	496	421
S/N Ratio (dB)	16.2	16.4	14.8	13.0	14.0	11.2	5.4	6.9

7.2.2 *General Comments about the Sources of Noise and Steps that could be taken to increase the S/N Ratio*

Radio Frequency (RF) noise is detected by the EMAT as it acts as an antenna. Noise can be detected if the EMAT is too close to an electrical device that emits RF. For instance, it was found that drive motors, some overhead sodium lights and a LeCroy oscilloscope could all interfere with the EMAT signal. When these electrical devices were switched off, then the noise disappeared. In a steel mill, it would be possible to screen as many nearby sources of noise as possible, for instance by moving electrical equipment and by screening the equipment.

The EMATs must also be electrically grounded to ensure they do not form part of an earth loop and a good quality, clean ground supply should be used.

As the EMATs have a metal case, they are electrically conductive. If they are clamped into position using metal holders, then these are also electrically conducting and these clamps themselves may be mounted onto a roller table which in a steel mill will be connected to many electrical devices. It was found via experimentation that one way to remove significant levels of noise was to ensure the EMAT was clamped in position using insulating parts such as ceramic washers and inserts, which were successfully tested at high temperatures.

A 1.9MHz low pass electronic filter is also used to remove frequencies above which the EMATs are not designed to detect ultrasound. These filters are used before the coaxial data cable is connected to the oscilloscope or high speed digitizer cards. The data could also be filtered using software in FPGA modules or with LabVIEW.

Signal averaging can also be used to reduce noise levels in the signal, although this is only practical on stationary steel.

7.2.3 *Steps Taken to Improve the Quality of Ultrasonic Signals at High Temperature*

Initial trials showed a significant decrease in the detected R-wave amplitude (Fig. 14) above the Curie point for the steel. A variety of different techniques were therefore used to enhance the received signals and solve the problem, which included:

- A new EMAT pre-amplifier was constructed for subsequent trials. The amplifier had an increased gain and a better signal to noise ratio.
- A thinner gauge wire (0.08 mm) was used in the EMAT detection coil. Initial tests used a wire with a diameter of 0.12 mm. This resulted in the EMAT coil having more turns, but the same width as in previous designs, which increased the sensitivity of the EMAT due to the larger coil inductance.
- A plano-convex lens was used to focus and decrease the laser beam diameter which increased the power density from 2.0 TWm^2 to 18.2 TWm^2 [21,34].

7.3 Additional Tests and Results Conducted at High Temperature

After these enhancements were implemented, more trials were performed on hot samples at Teesside Technology Centre. Results were obtained from 730 °C to room temperature and Fig. 15 shows some of these results plotted along the same axes.

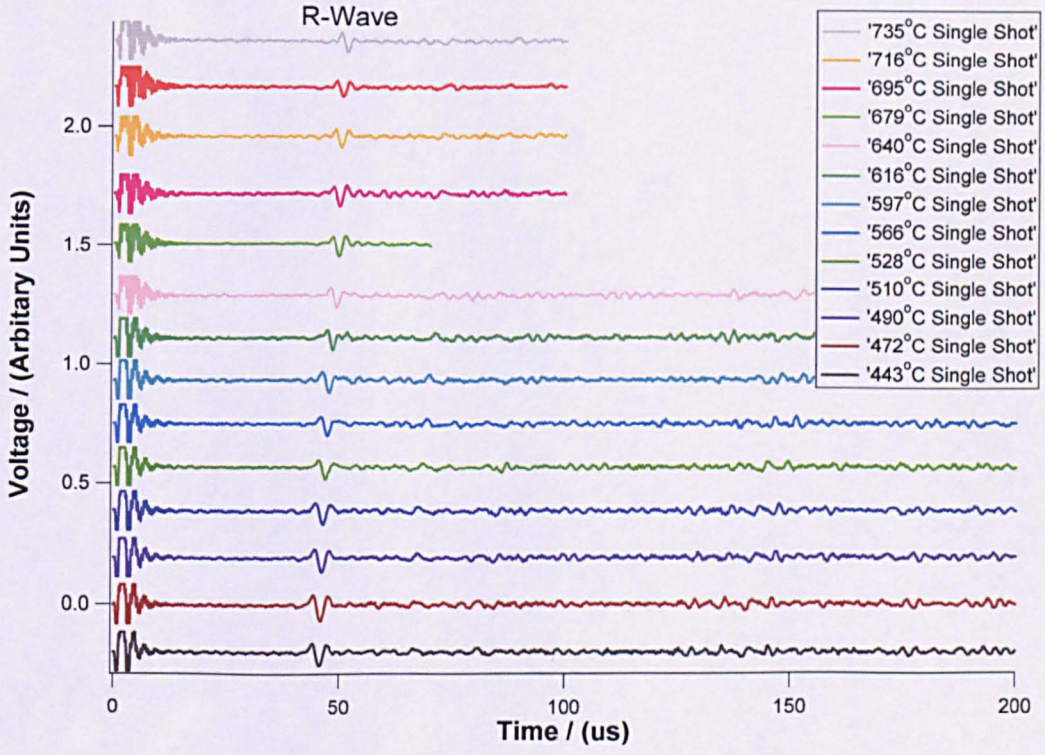

Fig. 15: Single shot A-Scans taken at a variety of different temperatures.

Table 4 shows higher S/R Ratios than those taken in previous trials, at a variety of different temperatures. It should be noted that this data is 'single shot' and therefore shot-to-shot variations when the laser beam hits the surface will affect the measurements. Table 5 shows the results that were recorded when the data was averaged, meaning that single shot variation is averaged out and that random noise is not being saved. This is reflected in the data presented in Tables 4 and 5 which show a higher S/N for averaged data.

Table 4

Table of S/N Ratios for A-Scans obtained at different temperatures for single shot data

Temperature (°C)	735	716	695	679	640	616	597	566	528	510	490	472	443
RMS Signal (Arbitary Units)	2278	1968	2357	2018	2523	2545	2723	2657	2303	2571	2807	2938	2671
STDEV Signal (Arbitary Units)	2280	1969	2360	2690	2524	2521	2719	2630	2303	2570	2808	2936	2672
RMS Noise (Arbitary Units)	253	240	208	284	285	271	297	228	225	296	252	283	282
STDEV Noise (Arbitary Units)	253	240	208	284	285	270	296	226	218	293	247	286	278
S/N Ratio (dB)	19.1	18.3	21.1	17.0	18.9	19.5	19.3	21.3	20.2	18.8	20.9	20.3	19.5

Table 5

Table of S/N Ratios for A-Scans obtained at different temperatures when the data is averaged

Temperature (°C)	679	640	616	597	566	528	510	490	472	443
RMS Signal (Arbitary Units)	2234	2335	2400	2527	2698	2377	2492	2531	2803	2799
STDEV Signal (Arbitary Units)	2472	2339	2381	2497	2532	2378	2493	2533	2802	2798
RMS Noise (Arbitary Units)	96	87	62	59	66	59	53	69	64	68
STDEV Noise (Arbitary Units)	95	86	55	48	59	49	43	59	55	58
S/N Ratio (dB)	27.4	28.6	31.7	32.7	32.3	32.2	33.4	31.3	32.8	32.3

Figure 16 compares two single shot A-Scans (from Fig. 15), one taken at 735 °C and the other at 443 °C. Here, it is possible to see how the change in arrival time of the R-wave varies with temperature. The shape of the R-Wave is different because the laser generation mechanism has been modified due to the increase in sample temperature and the attenuation and dispersion of the ultrasound may also have changed. It would be expected that the S/N ratio should increase with decreasing temperature, but by inspecting the single shot data in Table 5 and Fig. 16, this is not the case. However, when the data is averaged, the S/N ratio increases with decreasing temperature as expected. One reason the data does not perform as expected for single shot data could be shot to shot variation changes in the laser generation mechanism.

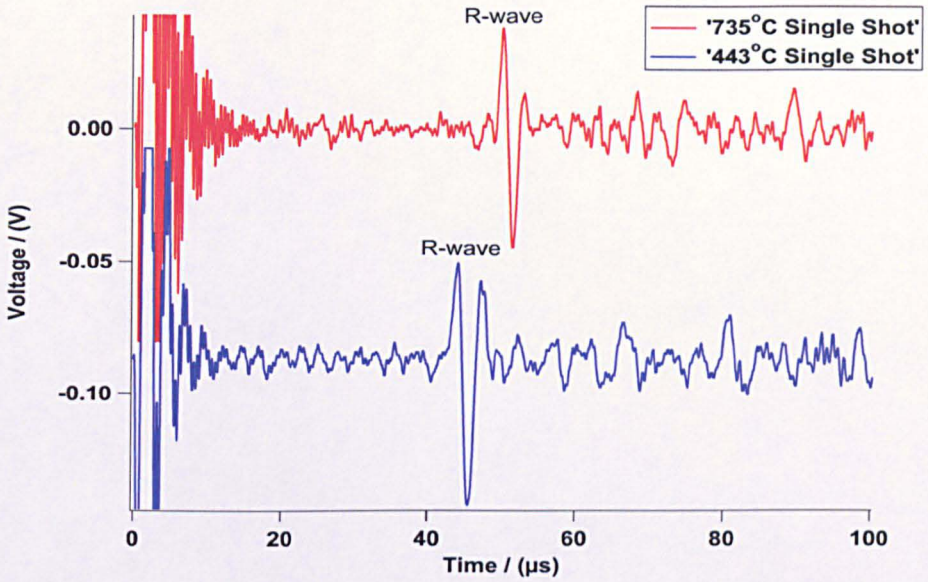

Fig. 16: Comparison between two single shot A-Scans, taken at different temperatures.

Figure 17 shows a graph comparing a single shot A-Scan with an A-Scan that was averaged 100 times at a temperature of 679 °C (the highest temperature where the data was averaged). Here, it can be seen that the comparison in terms of clarity between single shot and averaged data is very good and that both the P-wave and R-wave are easily distinguishable. For an on-line system, good quality single shot data would be needed as the steel is moving. The difference in arrival time between the single shot data and the averaged data can be attributed to the time taken to average the data and save it onto floppy disk using the oscilloscope. During this time, the billet was cooling and therefore the ultrasonic velocity was increasing during the measurements.

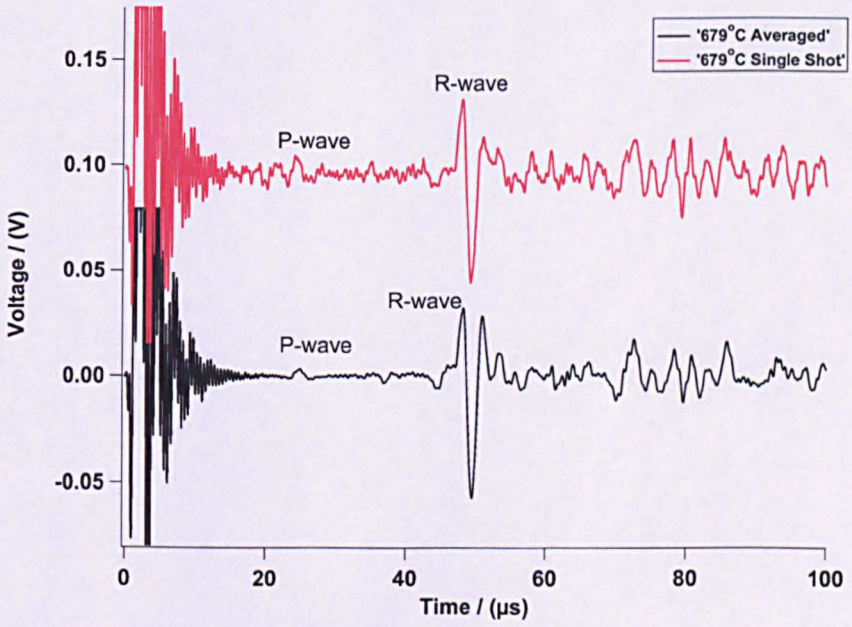

Fig. 17: Comparison between single shot and averaged data, taken at the same temperature during the trial.

Figure 18 shows a graph of Rayleigh wave velocity plotted against temperature. The velocity *(v)* was calculated by dividing the separation distance between EMAT *(d)* and laser by the arrival time *(t)* of the first maxima peak of the Rayleigh wave. Here, the velocities have been calculated from both the single shot and averaged A-Scan data. It should be noted that at the start of the experiment, no averaged data was recorded as the steel was cooling rapidly, hence the number of data points for the single shot data is not the same as those for the averaged data. For both sets of data, the r^2 value has been calculated by plotting a least squares fit line through the data using Microsoft Excel. Here, r^2 is calculated by dividing the variance from regression (SSR) by the variance from data (SST), as denoted by the equation below:

$$R^2 = \frac{SSR}{SST} = \frac{\sum_1^n (\hat{y}_i - \bar{y})^2}{\sum_1^n (y_i - \bar{y})^2} \qquad \text{(Equation 7.4)}$$

The error bars are calculated by considering the error in the temperature and velocity measurements. The error in the temperature measurement is very low, as Type K thermocouples exhibit an error level of around 0.75%[44]. However, the largest error when measuring the temperature is the length of time taken to look at the reading and save the waveform data to disk, which can be up to 15 seconds when data is being averaged. Therefore the error in temperature measurements was taken to be ± 10 °C. The error in the velocity value is dependent upon the errors in measuring the distance between laser beam and EMAT coil and the arrival time (*t*) of the R-wave. The distance between the centre of the laser beam and centre of the coil has an error, (Δd) to within ± 2 mm. The steel will also be contracting slightly as it is cooling which may affect the absolute distance between laser beam and EMAT receiver. The error in the arrival time (Δt) is dependent upon how the arrival time is measured. In this case, every arrival time from each A-Scan for all the different temperatures was taken from the same point, i.e. the first maximum on the R-wave sampled data. This maximum point is dependent upon the number of points in the R-wave peak and can therefore have a time error (Δt) of ± 20 ns. Therefore the error in the velocity (Δv) can be calculated by:

$$\Delta v = v \cdot \left[\left(\frac{\Delta d}{d} \right)^2 + \left(\frac{\Delta t}{t} \right)^2 \right]^{\frac{1}{2}} \qquad \text{(Equation 7.5)}$$

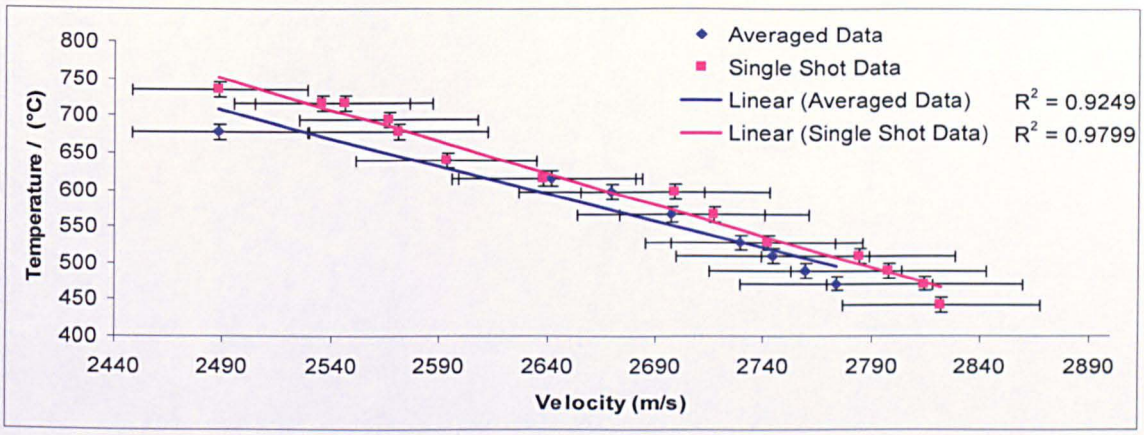

Fig. 18: Graph of temperature against Rayleigh wave velocity, for both the averaged and single shot A-Scan data.

Figure 19 shows the graph of P-wave velocity plotted against temperature, where the time data were extracted from the averaged A-Scan data (for some of the single shot data, the P-wave was indistinguishable from background noise). The errors were calculated as for the R-wave calculations.

Because the velocity of the ultrasonic waves varies with temperature, it will be necessary for an on-line system to be able to use the appropriate calibration velocity in any calculations to determine the expected arrival times of the waves. This would be relatively straightforward for predicting the arrival time of the P-wave and R-wave. Should waveforms not arise when expected, then this could mean that a defect is present and is blocking the ultrasonic path. It is more complex to predict bulk wave arrival times in hot steel as there is a steep temperature gradient in the steel product. Experiments conducted for this project showed that thermal imaging temperature measurements of the steel surface correlate well with surface temperatures of as-cast semis predicted using Finite Element Models (FEM)[6]. These same models also predict what the internal temperature gradient is and therefore there is some confidence that the arrival times of bulk waves can be correctly predicted. Through experiment, it should be possible for an on-line system to determine the approximate temperature of the product being inspected through the use of an optical pyrometer and the arrival time of the Rayleigh wave and use this in connection with models to predict the internal temperature gradient.

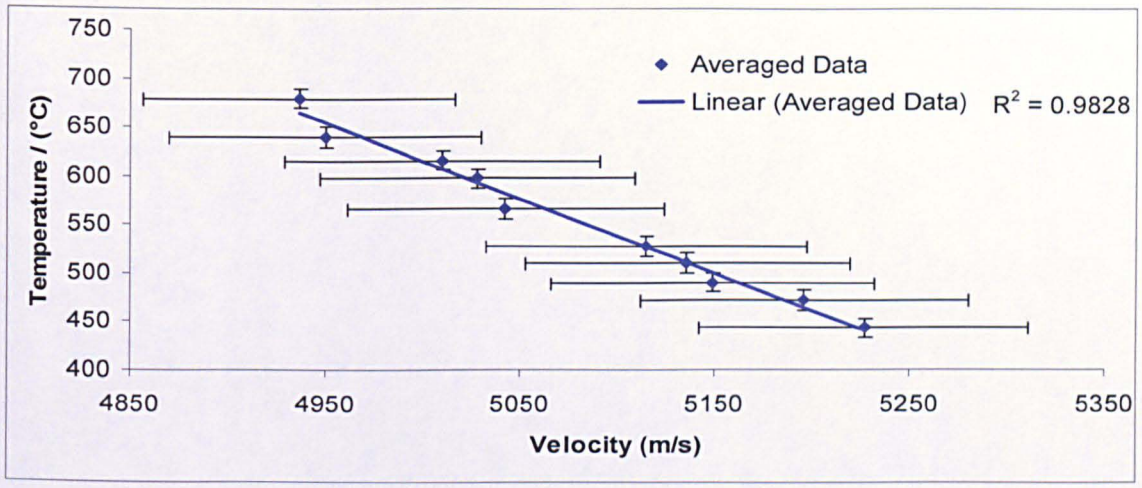

Fig. 19: Graph of temperature against P-wave velocity,
for both the averaged and single shot A-Scan data.

7.4 Summary

The water-cooled EMAT and experimental arrangement allowed good quality, single shot data to be obtained at elevated temperatures. The EMAT successfully survived the trial. These measurements demonstrated that the technology was suitable for further developments such that it would be used for testing hot, moving steel.

8. DEVELOPMENT OF AN AUTOMATED INSPECTION SYSTEM

8.1 Construction of a Mechanical EMAT Holder to Accommodate Variability in Product Thickness

An EMAT holder was designed and built to accommodate the Laser-EMAT system inspecting steel with different thicknesses. Additionally, the holder was designed to solve the problem whereby the product thickness can vary by a few millimetres during the continuous casting process, when the dimensions of the steel can change due to the conditions in the casting mould and forces exerted on the strand from the withdrawal rollers. Additionally, this mechanical EMAT holder was designed to ensure a near constant stand-off above moving steel. Another problem, whereby steel semis move up and down when passing over rolls also needed to be solved. Therefore, because the stand-off between the EMAT and the billet could change rapidly, a solution involving a pantograph design was validated through experimentation to ensure a near constant stand-off.

This comprised of a skid in which the EMAT could be held as can be seen in the schematics of Figs. 20a and 20b.

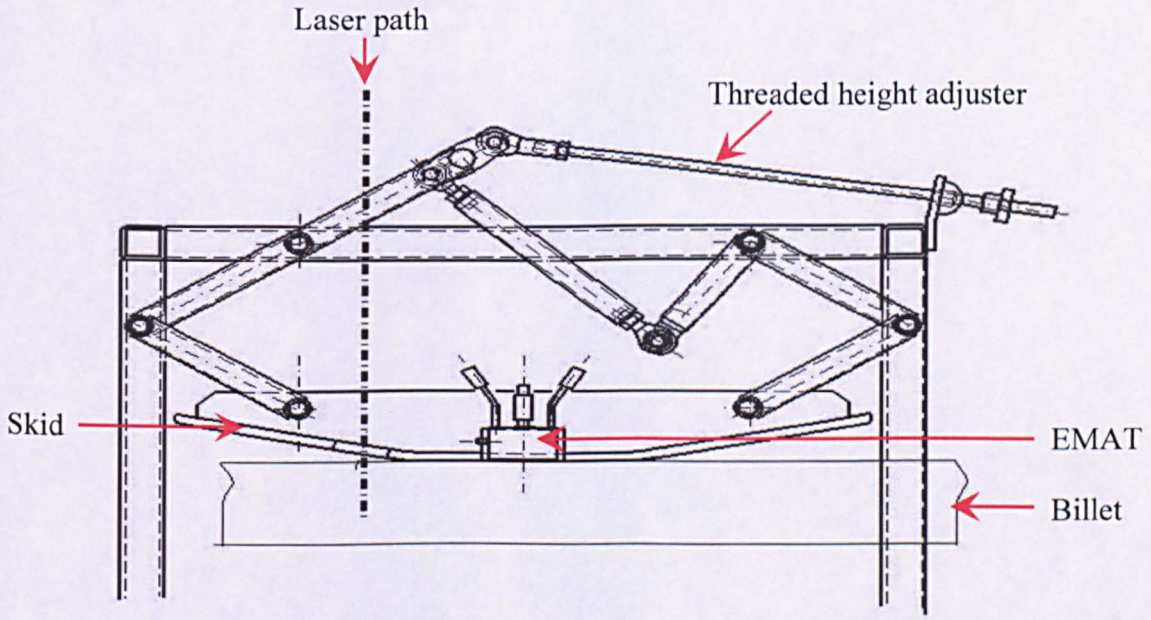

Fig. 20a: Side view of the EMAT pantograph.

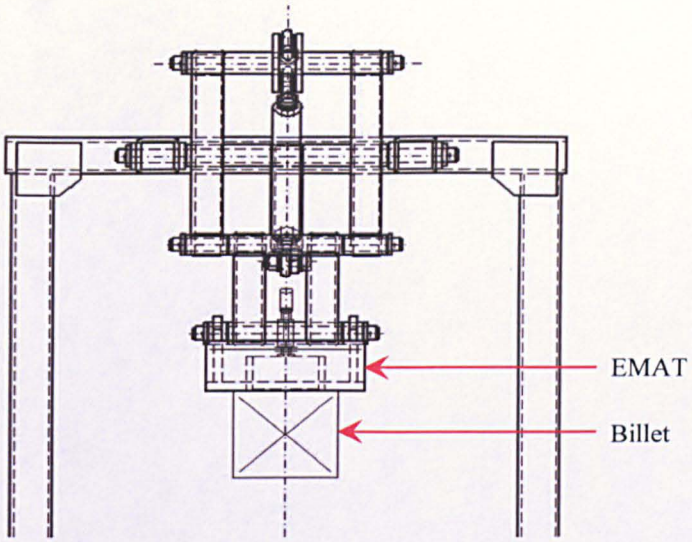

Fig. 20b: Front/exit view of the EMAT pantograph.

A photograph of the pantograph being used in the Pilot Rolling Mill can be seen in Fig. 21. Here, the skid/EMAT was successfully kept parallel to the steel surface. This was confirmed by looking at video footage of the trial. Because the steel would be travelling backwards and forwards in the Pilot Rolling Mill, a method to ensure the EMATs could be automatically positioned on top of any hot steel semi was achieved by using a skid that was angled at both ends. When the semi was moving and hit the skid, it was knocked upwards and then dropped down onto the top face of the steel. Because the skid is angled at both ends, the steel can be fed through the pantograph from both directions. This meant that for rolling mill trials, billets could be passed backwards and forwards underneath the EMAT holder. The skid was made from hard wearing carbon steel and was designed to be robust and long standing.

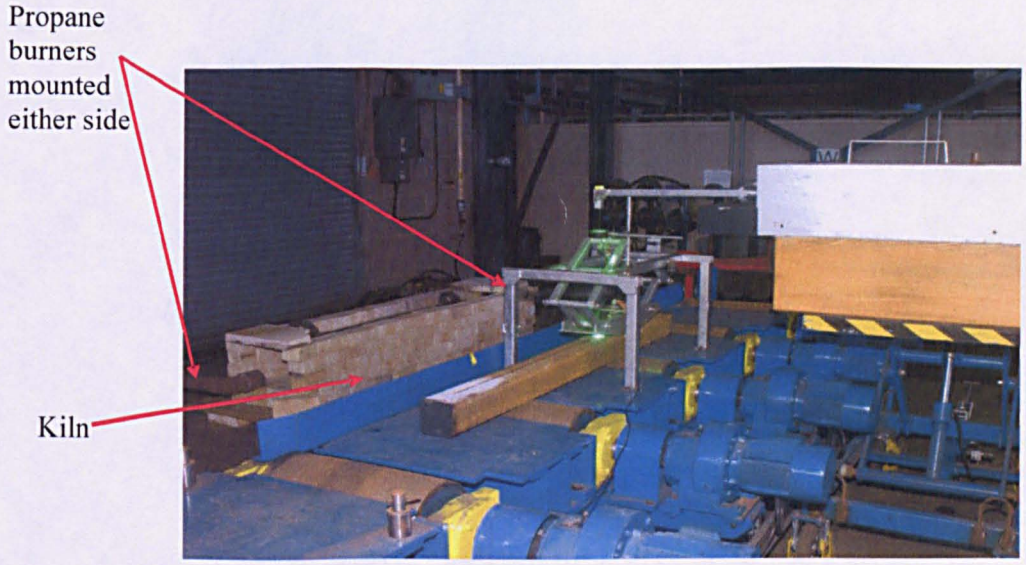

Fig. 21: Billet being inspected at room temperature,
using the Roller Straightener Mill at Teesside Technology Centre.

8.2 Constructing a New, Dedicated Data-logging PC

Significant amounts of data were required to be saved rapidly to a PC's hard disk during trials as part of this project. To solve this problem, a data-logging PC was designed and built. This PC had a motherboard with 5 PCI slots, 3 of which were occupied with 2-channel National Instruments high-speed digitiser cards, to simultaneously acquire data from up to six EMATs. This motherboard also contained SATA interfaces allowing RAID-0 hard disks to be used. At the time, these disks were the fastest way to save data. Additional fan cooling to keep the system operational was also installed.

Because each A-Scan is 80 kb in file size, when the laser operates at 20 Hz, 1.6 Mb of data needs to be written to disk every second for each EMAT. Therefore if the maximum array size of 6 EMATs is used, 9.6 Mb of data needs to be written to disk every second. New LabVIEW software was written to save the data in National Instrument's proprietary TDMS and TDM format, which was found to be the fastest method of successfully writing large quantities of data (that is compressed) to disk.

It should be noted that the 80 kb file size is recorded using the highest possible sampling rate that the digitiser cards can acquire so that good quality signals can be achieved. For a plant based system, this file size would be significantly smaller. For example, 40,000 points of data are recorded in every A-Scan and this number could be significantly reduced. Similarly, data arriving from before the P-wave could be ignored. Having smaller file sizes would mean saving disk space and increase the speed of subsequent analysis. Typical computer screen resolution is 1280 x 800 pixels and therefore B-Scans should be optimised for this type of display output. However, for this project, as the capacity to save and analyse data was feasible, the highest possible sampling rates were used.

8.3 Construction of an Automated Trolley Inspection System

A system was required to test billets under laboratory conditions in order to develop the Laser-EMAT system and to ensure it could work on moving steel. This needed to be done in a controlled manner prior to installing the Laser-EMAT system on the Pilot Rolling Mill, whereby any potential problems could be identified and rectified prior to a costly installation process. In order to solve this problem and move long, heavy steel billets weighing up to 250 kg in a series of very accurate steps, a conveyor belt system was designed and built[6]. This moving conveyor was mounted on top of a support frame on wheels to form a trolley. The pantograph frame holding the EMAT was moved onto the trolley system and this frame was equipped with a lens holder so as to focus the laser beam onto the steel surface to help optimise the Laser-EMAT system. This system can be seen in Fig. 22.

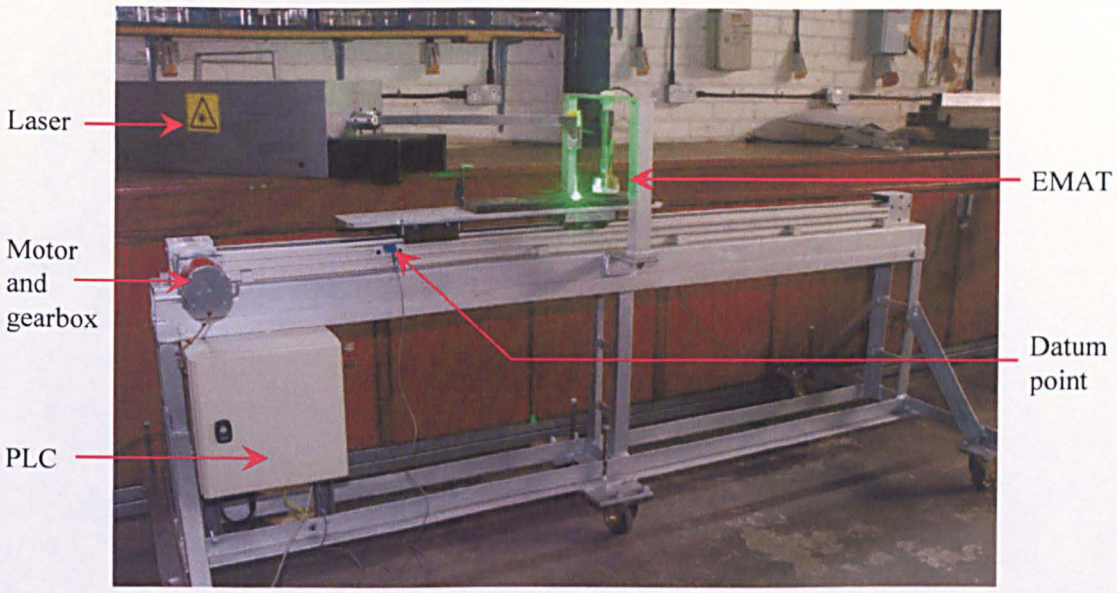

Fig. 22: The automated trolley system. Here, a LabVIEW program was used to fire the laser, move the steel and acquire the EMAT data.

The trolley system used a servo-motor that moved a carriage mounted on the conveyor to within micron accuracies. The system was designed to move steel samples in increments as small as 0.1 mm.

LabVIEW software was written to start the carriage at the zero (datum point) position which was a condition reached when the carriage carrying the steel moved to a position where a sensor was mounted.

The LabVIEW software was also written to not only move the steel sample, but to also fire the laser, acquire the EMAT data and save the data to disk. This demonstrated the potential for a fully computerised on-line control system.

9. ON-LINE SURFACE DEFECT DETECTION ON HOT, MOVING STEEL

One of the problems with installing new equipment on a steel plant is anticipating what results to expect. It was not known what would happen when the Laser-EMAT system was first used to test hot, moving steel. Therefore the following sections show that confidence was gained testing the Laser-EMAT system on moving steel at room temperature. This allowed any practical issues to be resolved before inspecting hot steel so that the performance when the steel was hot and moving could be anticipated.

9.1 Experimental Method

A 1.6 m long, 110 mm square steel billet with a simulated, milled, 4 mm deep transverse defect was inspected under a variety of different laboratory conditions before heating and inspecting the same billet at temperatures of over 800 °C.

Ultrasonic methods can be used to find defects in moving steel. An example of a manufacturing problem, whereby a transverse surface defect is in the middle of the top face of a billet is presented in this section. Here a billet was moved from left to right underneath the fixed inspection point of the Laser-EMAT system. More in-depth details of this trial can be found in Engineering Doctorate Submission Number 4[6].

The following trials were conducted:

(i) The LabVIEW controlled trolley system discussed previously, moved the billet over very accurate distances so that one face along the length could be inspected ultrasonically, in increments of 2 mm. These results were then compared against results from a Finite Element Model to help identify features visible in the recorded waveforms.

(ii) The trolley system was then used to inspect the moving billet moving at a constant velocity. This measurement was taken under laboratory conditions, so that it would be possible to ascertain what to expect when the equipment was moved to the Pilot Rolling Mill.

(iii) The same billet was then inspected on the Pilot Roller Mill at Teesside Technology Centre. Here, the steel was moved back and forth under the Laser-EMAT system. This was to ensure that measurements were comparable with those listed in (ii) and to ensure the equipment was ready for conducting tests on the heated steel billet.

(iv) After these tests were conducted, the billet was then heated in a kiln, before being positioned on the rolling mill and moved back and forth under the Laser-EMAT system. This was essentially a repeat of experiment (iii), but conducted on a billet heated to 1200 °C and inspected when the surface temperature was over 800 °C.

By testing the same billet under each of these different conditions, the results can be correlated with the geometry of the experimental arrangement. Using trigonometry, it is possible to predict the arrival times of the various ultrasonic waves when no defects are present. The effect that the presence of simple geometric shaped defects will have on the waveforms can also be predicted. A Finite Element Model was compared to the results obtained experimentally.

9.2 How the Presence of a Surface Defect Can Affect Ultrasonic Signals

The transverse surface defect was found by considering three cases explaining where in relation to the defect the laser and the EMAT were when the billet was moved from left to right.

9.2.1 Case 1 - The Laser-EMAT System is to the Right of the Defect

When the laser beam and EMAT are both positioned to the right of a defect (i.e. no defect is blocking the path between laser and EMAT as in Fig. 6a), the direct R-wave and P-wave are detectable. The R-wave has a relatively large signal amplitude. The R-wave will also be reflected from the slot. As the defect moves closer to the Laser-EMAT position, the arrival times of the reflected R-wave will occur progressively earlier. The R-wave will also be reflected from the right-hand edge of the billet and this will take longer to reach the Laser-EMAT, the further the billet moves from left to right.

When the sensitive coil of the EMAT is within a few millimetres of the defect, the reflected waves constructively and destructively interfere with the direct R-wave, leading to a significant increase or decrease in the measured signal amplitude[18].

9.2.2 Case 2 - The Defect Lies Between the Laser and the EMAT

When the defect lies between the laser beam and the EMAT, as shown in Fig. 6b, the direct Rayleigh wave will be at least partially blocked. The R-wave may not be detectable if the defect is significantly deeper than the wavelengths present in the wideband R-wave as most of the energy associated with the R-wave is bound within a depth of 15 mm from the surface. There may still be some evidence of the R-wave if the defect is shallow (e.g. 4 mm deep), as lower frequency components of the wideband R-wave can in part propagate more readily underneath the defect[18].

At the defect, a fraction of the P-wave energy will be mode converted into an R-wave and similarly, a fraction of the R-wave will be mode converted into a P-wave thereby creating a distinctive "x" shape in the B-Scan, which is shown in Section 9.3.2. The P-wave may not be detectable immediately after the crack. This is because the P-wave is the surface manifestation of a bulk longitudinal wave and whilst the crack can reflect some of this incident energy, energy can also leak out from the propagating bulk wave wavefront towards the surface.

Other results that can be attributed to the presence of a defect are discussed earlier in Section 6.3.

9.2.3 Case 3 - The Laser-EMAT System is to the Left of the Defect

Case 3 can be seen in Fig. 6a where the path between the laser beam and EMAT is not blocked by the defect.

9.2.4 General Observations

When the R-wave is Fast Fourier Transformed (FFT), the maximum peak value of the magnitude FFT of the R-wave will drop by several kHz if a defect is blocking the path between the laser beam and EMAT. This is because the defect acts as a filter and attenuates the higher frequency signals. This is detailed further in Section 9.3.4. The drop in frequency content is another method employed for locating and gauging defects[18].

Bulk waves that travel from the top of the billet into the bulk of the billet are reflected off the bottom surface, back to the top surface and will remain unaffected by the presence of surface defects on the top surface of the billet. However, if surface defects are present on the bottom surface of the billet the waves can be diffracted from the crack tip, which means that defects on the bottom face of the steel can potentially be detected using this approach, as detailed later in this report in Section 10. If any internal defects exist, then the arrival times of the ultrasonic waves may occur earlier or later than would otherwise be the case, or may not be detected at all.

9.3 LabVIEW Controlled Trolley System to Inspect an Incrementally Moving Billet Sample at Room Temperature

9.3.1 Experimental Arrangement

Here, the billet was moved through a total distance of 1200 mm in 2 mm increments under the fixed position of the Laser-EMAT system. The more powerful, but non-portable 1064 mm laser system was used for this trial. Sixteen waveforms were taken at each of the six hundred different movement positions of the billet, which were then averaged to give six hundred averaged A-Scan readings for each inspection point along the billet. The data were acquired at a digitisation rate of 200 MHz.

9.3.2 Results

The characteristic differences in waveform appearance, when a defect is or is not present can be seen in Fig. 23. This shows averaged data from two A-Scans, one for Case 1 conditions where no defect is blocking the path of the R-wave (which is the same for Case 3) and for Case 2, where the signal amplitude of the R-wave has dropped and the frequency content has changed. The P-wave, R-wave and SS-wave have all been identified in Fig. 23. It should be noted that the reflected R-wave (and the other reflected mode converted surface waves) can interfere with the bulk waves arriving at the surface of the detector, therefore resulting in a change in the measured signal amplitude.

A LabVIEW program was used to construct a matrix with 600 columns, representing the 600 different positions of the moving billet, where each column contained the averaged voltage readings for each A-Scan. The matrix comprised 40,000 rows, which was the number of points recorded for each A-Scan and the entire matrix was formatted as a TDM file. This matrix was used to make an image plot, called a B-Scan. Here, the B-Scan is comprised of an x, y and z-axis. The x-axis is the time and this is dependent upon the digitiser acquisition rate and this is a constant for each A-Scan, i.e. all A-scans range from 0 μs to 200 μs and therefore the x-axis of the B-Scan ranges from 0 μs to 200 μs. The y-axis is the distance through which the billet

has been moved, which in this case was between 0 mm and 1200 mm. The z-axis is a colour representing each of the 40,000 points comprised in every A-scan.

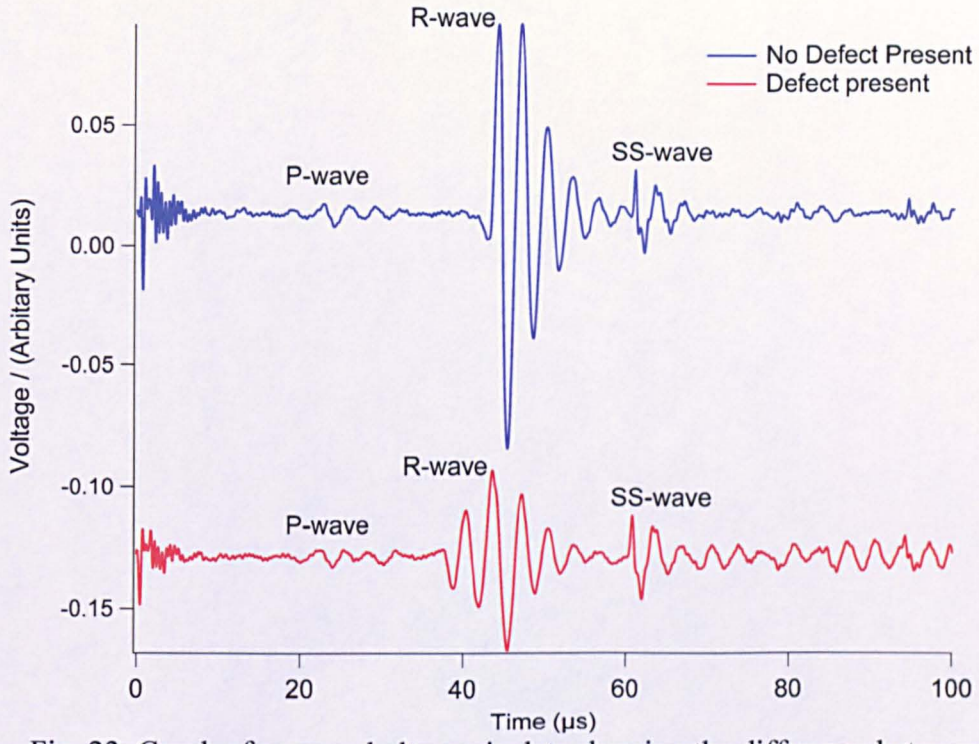

Fig. 23: Graph of averaged ultrasonic data showing the difference between whether or not a defect is present.

A B-Scan was plotted containing the data from this TDM file and can be seen in Figs. 24a and 24b. Here, Fig. 24a has several regions of interest highlighted and these features can be seen more clearly in Fig. 24b where the labels have been removed for clarity. Regions [a] and [b] in Fig. 24a correspond to the location of the defect which attenuates the surface waves and this is magnified and shown in more detail in Fig. 24c. Regions [c] and [d] show the signal that corresponds to the R-wave being reflected from the defect. Region [c] is the reflected wave from the defect from Case 1. The reflected wave from Case 3 can be seen in Region [d]. Regions [e] and [f] show a R-wave being reflected from the billet edge.

Figure 24c contains two other waves of interest, [m] and [n]. The feature in region [m] corresponds to a surface-skimming P-wave that has mode-converted to a R-wave at the crack tip and the feature in region [n] corresponds to an R-wave that has mode-converted to surface-skimming P-wave. Region [b] shows the drop in R-wave signal amplitude when a defect blocks the path between the laser and EMAT. There is also a small delay in the arrival time of the R-wave, compared to the A-Scans either side of the defective region, which can be attributed to the presence of the defect. (Some of the horizontal lines that occur in the B-Scan can be attributed to electromagnetic noise from the motor.)

Looking at the results in Figs. 24b and 24c, both the P-wave and R-wave are evident, even when the slot is blocking the path between the laser and the EMAT. This is due to some of the wideband R-wave propagating under the 4 mm deep defect. This means that not all of the surface waves are completely blocked by the defect, as it has been shown that longer wavelengths are able to pass under defects more readily than shorter wavelengths[18]. This was

confirmed by conducting FFT analysis on the recorded R-waves. If the defect had been deeper (e.g. >10 mm) then the R-wave would not have been detected at all.

A LabVIEW program was used to extract the R-wave from each A-Scan and magnitude Faster Fourier Transform the corresponding signal.

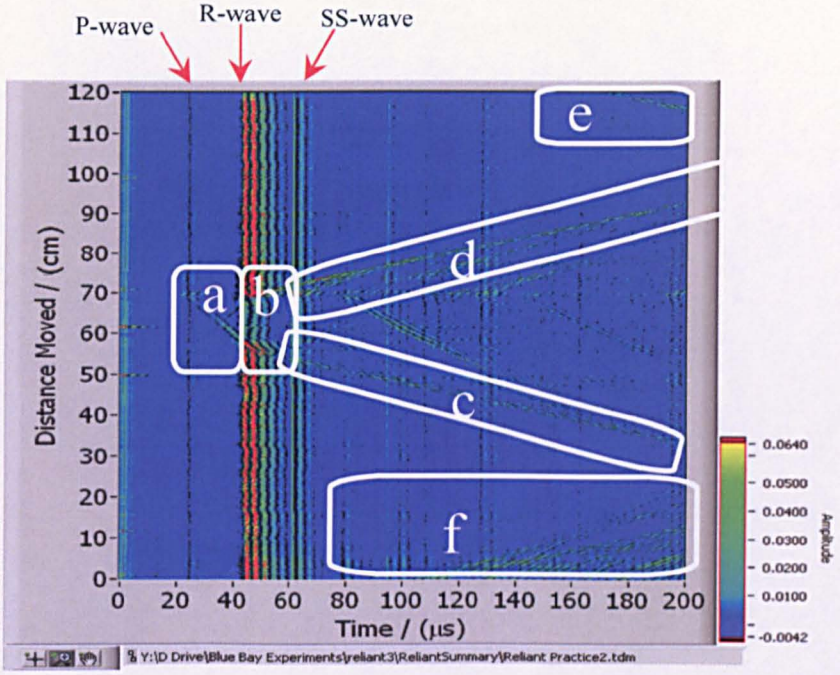

Fig. 24a: B-Scan for when the trolley moves in 2 mm increments, with regions of interest highlighted.

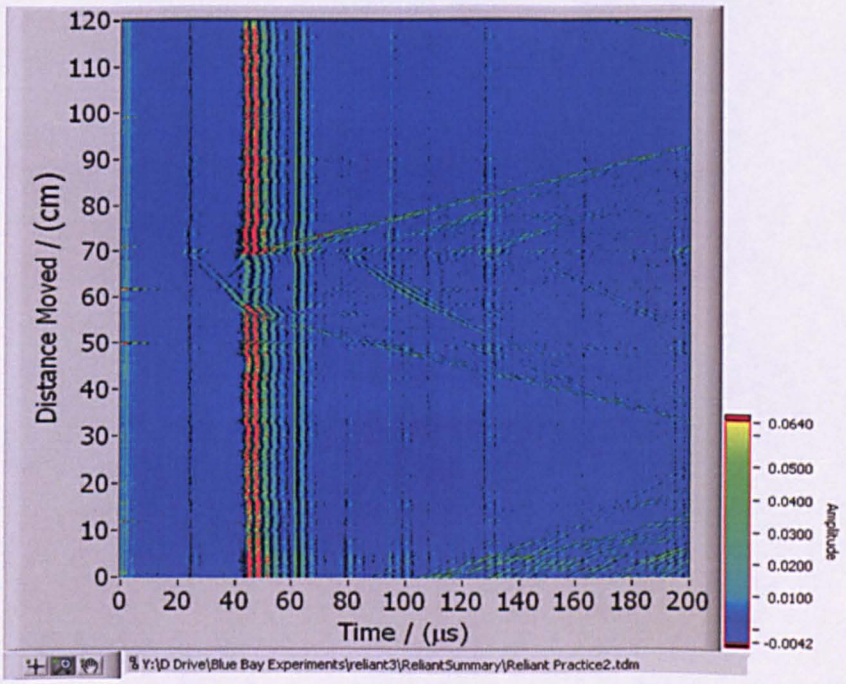

Fig. 24b: B-Scan for when the trolley moves in 2 mm increments.

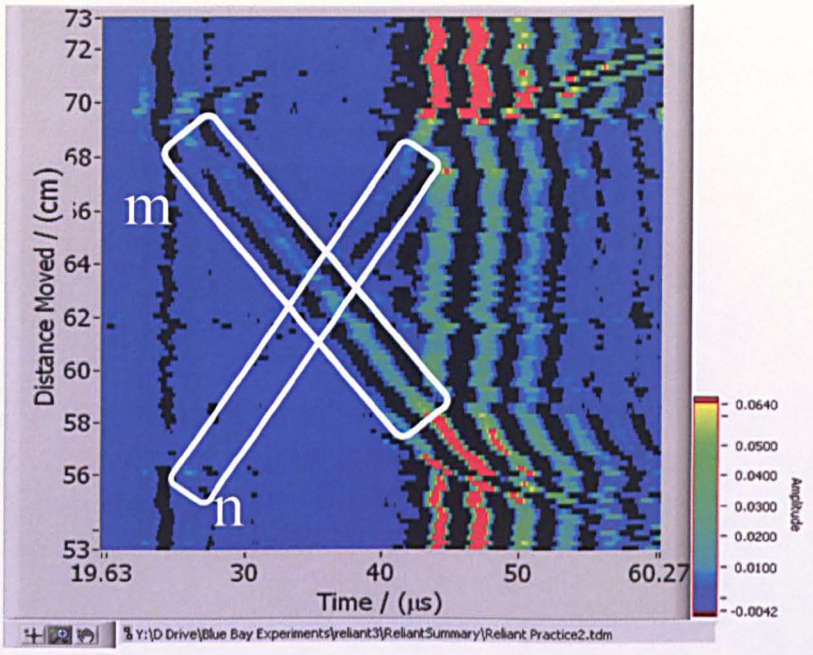

Fig. 24c: A magnified section of the B-Scan, highlighting the defect.

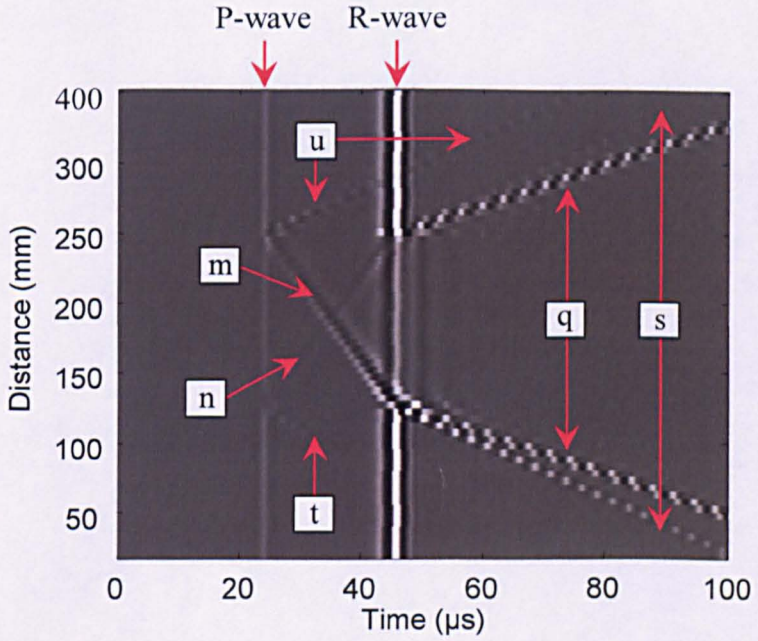

Fig. 25: A simulated B-Scan, calculated using FEM.

Figure 26 shows the position in frequency space of the maximum point on the magnitude FFT of the R-wave plotted against A-Scan number. Therefore another method to detect whether or not a defect is present is by looking for a noticeable decrease in the higher frequency content of the signal.

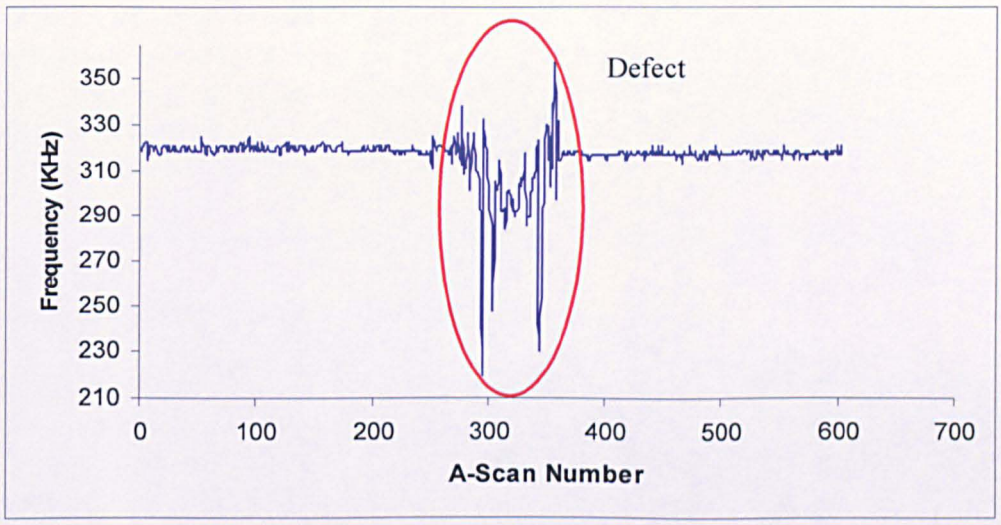

Fig. 26: Graph showing the position in frequency space of the maximum point on the magnitude FFT of the R-wave plotted against A-Scan number.

9.3.3 Comparison with Modelled Results

A Finite Element Model (FEM) was constructed by X Jian at The University of Warwick to plot a B-Scan based on the dimensions given from these experimental trials. This modelled the in-plane particle velocity in steel, as detected by the EMAT, from the R-wave generated by the pulsed laser beam. The FEM calculates the predicted arrival times for the various wave modes and plots a B-Scan. The simulated B-Scan can be seen in Fig. 25, which compares favourably with the B-Scan found experimentally, i.e. Fig. 24b.

The features in Fig. 25 have been labelled and can be identified as:

- Feature [q], which corresponds to the R-waves as they are reflected from the defect.
- Feature [s], which is an R-wave mode converted to a surface-skimming P-wave.
- Features [t] and [u] which are P-waves that have mode converted to R-waves[45].
- Feature [m] is a P-wave that has mode-converted to an R-wave at the crack tip.
- Feature [n] is an R-wave that has mode-converted to a P-wave.

9.4 Additional Tests to Move the Billet at a Constant Velocity

The automated trolley system was also used to move the billet at a constant velocity. Again, the defect was easily detectable from the B-Scan and FFT magnitude[6].

9.5 Pilot Rolling Mill System to Inspect a Moving Billet Sample at Room Temperature

9.5.1 Experimental Arrangement

The same billet was then moved along the rolls on the Pilot Roller Mill at Teesside Technology Centre a number of times to ensure the results were repeatable using the portable 532 nm pulsed laser system to generate the ultrasonic signals. The equipment used in this trial can be seen in the photograph of Fig. 21. Here, the defect was still clearly detectable when the data were analysed when using the less powerful, 532 mm laser system[6].

9.6 Pilot Rolling Mill System to Inspect a Moving, Hot Billet Sample

9.6.1 Experimental Arrangement

The billet that had previously been tested at room temperature on the rolling mill was heated to over 1200 °C in a refractory brick kiln and lifted by a crane into position before the inspection process began. By the time the billet was correctly positioned, it had already cooled significantly and the first set of ultrasonic measurements was taken at a surface temperature of 850 °C. A thermal imaging camera was used to measure the billet temperature. A photograph of the hot billet being inspected can be seen in Fig. 27.

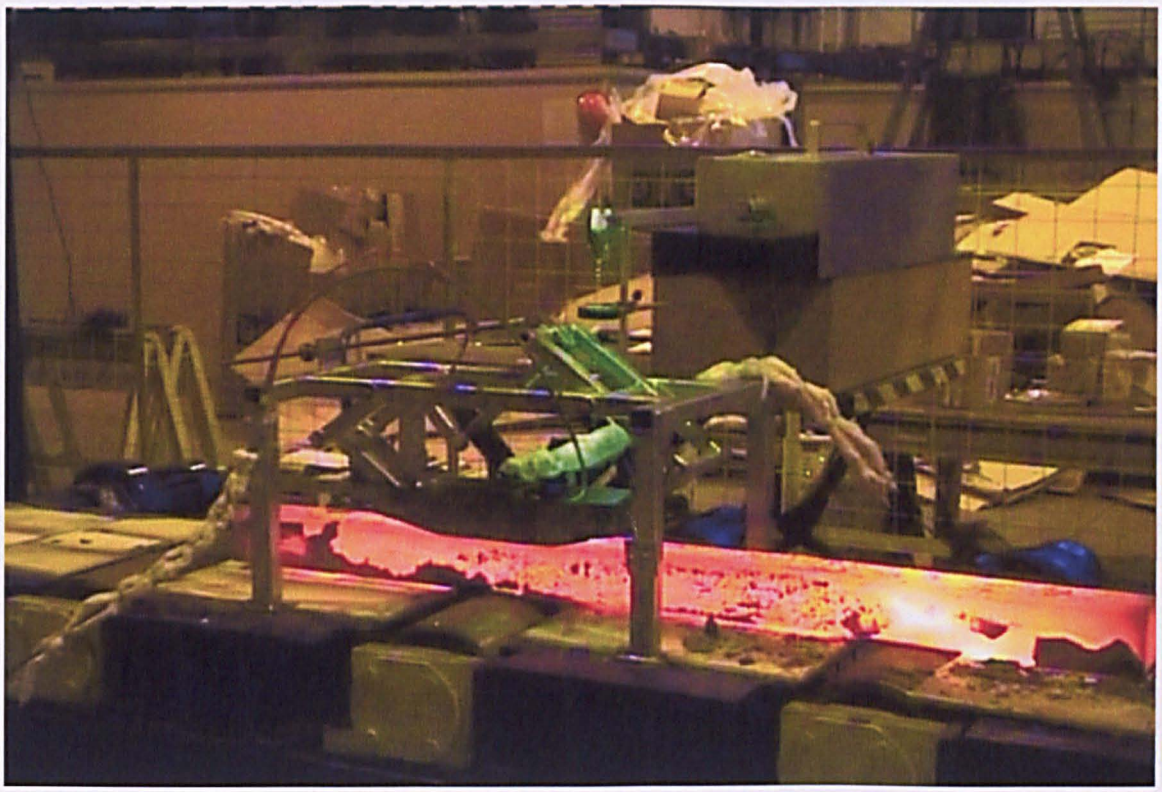

Fig. 27: Photograph of the hot billet under inspection.

9.6.2 Results and Discussion

B-Scan results taken at 850 °C on the moving billet can be seen in Fig. 28. Region [a] shows the presence of the defect as indicated by the drop in signal amplitude. The signal-to-noise ratio of the A-Scans was very poor and therefore a rolling average algorithm was used to clear up the data. Single shot A-Scan data from this trial can be seen in Fig. 29. This figure also shows how the A-Scans change when a defect is present.

It can be seen from Figs. 28 and 29 that a transverse defect can be detected above the Curie temperature of the steel using Laser-EMAT technology. The ultrasonic bulk waves that were detectable at room temperature were not detectable above the noise level beyond the Curie point.

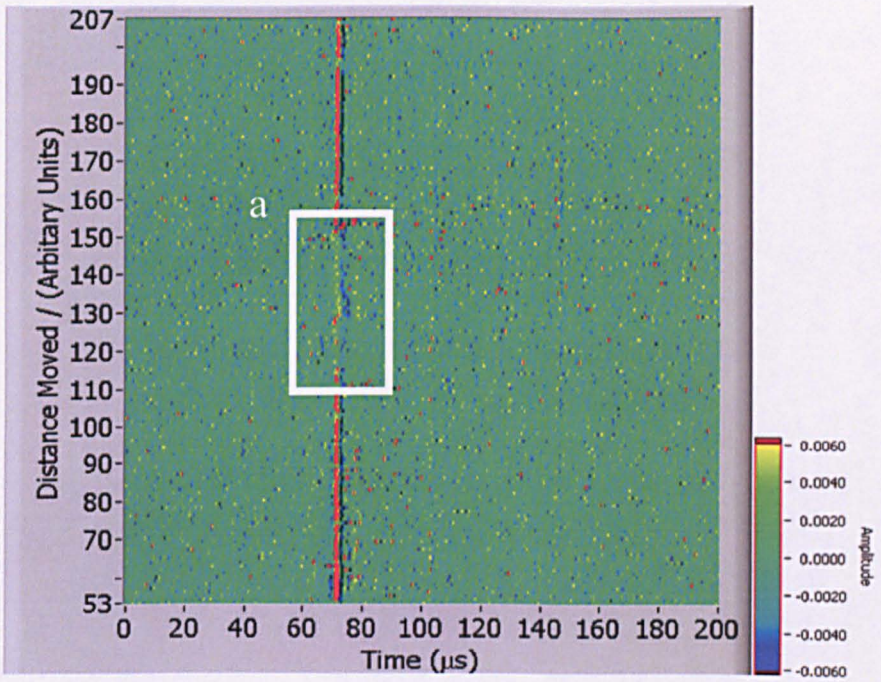

Fig. 28: B-Scan of the billet moving at 850 °C, on the pilot plant rolling mill.

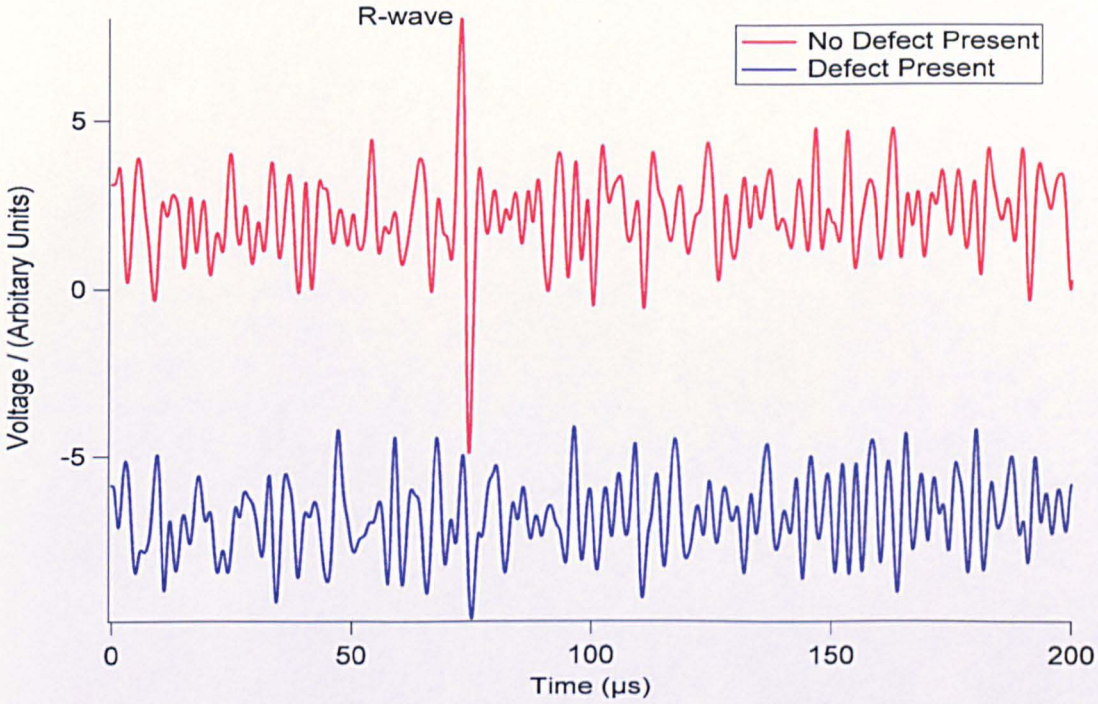

Fig. 29: Comparison of two single shot A-Scans, taken at 850°C that indicates the amplitude change when a defect is present.

9.7 Recommendations for Further Work to Improve Measurements at Elevated Temperature

Further work is needed to improve the signal-to-noise ratio of the detected ultrasonic signals, which will in turn improve the B-Scan resolution. The industrial robustness of the system is very good; the same EMAT survived repeated hot temperature measurements from the moving tests and suffered no noticeable deterioration in performance. A more powerful, portable laser system is recommended to increase the amplitude of the ultrasonic signals. This would increase the signal-to-noise ratio of the received ultrasonic waves and could also generate bulk waves with larger amplitudes. The water-cooled EMAT and specially designed EMAT holder ensure a near constant stand-off and this arrangement was proven to be mechanically sound. The data acquisition systems and subsequent data analysis showed that the ultrasonic data could be converted into meaningful B-Scans, utilising a high degree of automatic B-Scan plotting using LabVIEW software which was then used to show the location of a defect.

10. DETECTING DEFECTS ON THE BOTTOM FACE OF THE BILLET, WITH THE LASER EMAT EQUIPMENT MOUNTED ON THE TOP FACE

A trial was conducted using the automated trolley system to move a 2 m long billet a total distance of 600 mm in 1 mm increments. This billet had a transverse surface defect on the bottom face. The laser and EMAT were both mounted on the top face and held stationary as the billet passed underneath. The data were averaged 16 times in each position of movement and the resulting B-Scan can be seen in Fig. 30a. This shows the SS bulk wave and associated reflections from the defect that show a distinctive parabola shape bending away from the defect[25]. A magnified area, showing a drop in signal amplitude for the SS bulk wave when a defect is present can be seen in Fig. 30b. This demonstrates that the equipment can be used to find defects on the bottom face, even though the sensors are mounted on the top face. EMATs used specifically for internal inspection would require a much wider coil and also need higher frequency amplifiers.

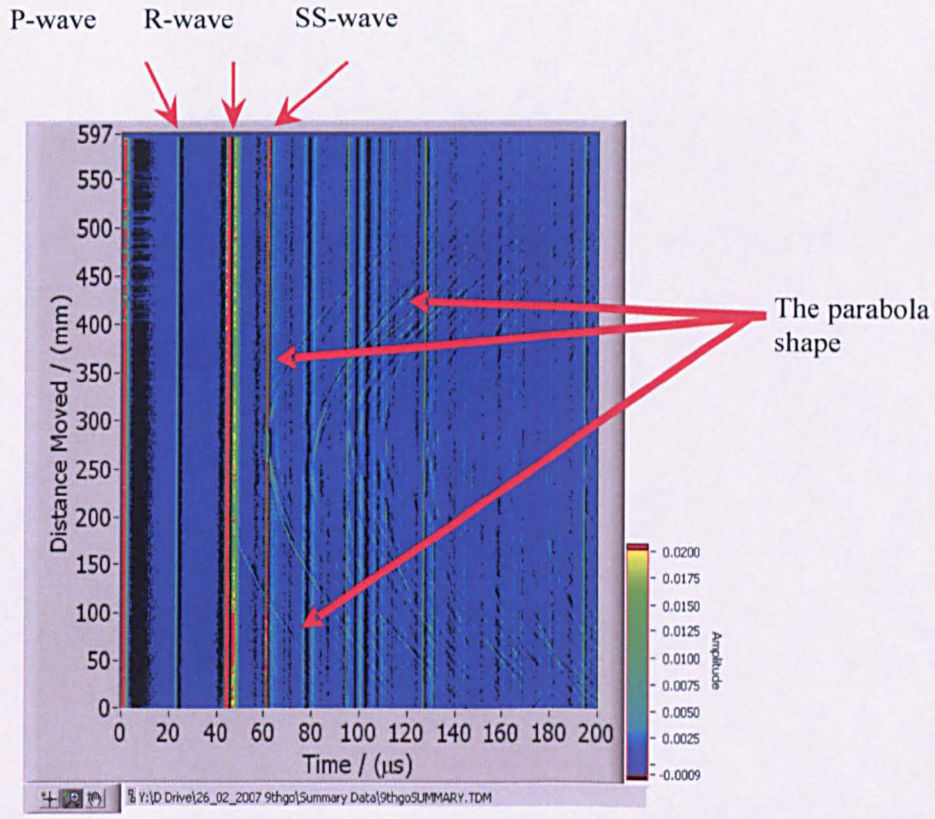

Fig. 30a: B-Scan showing the energy drop to the SS bulk wave and the reflections from the later bulk waves.

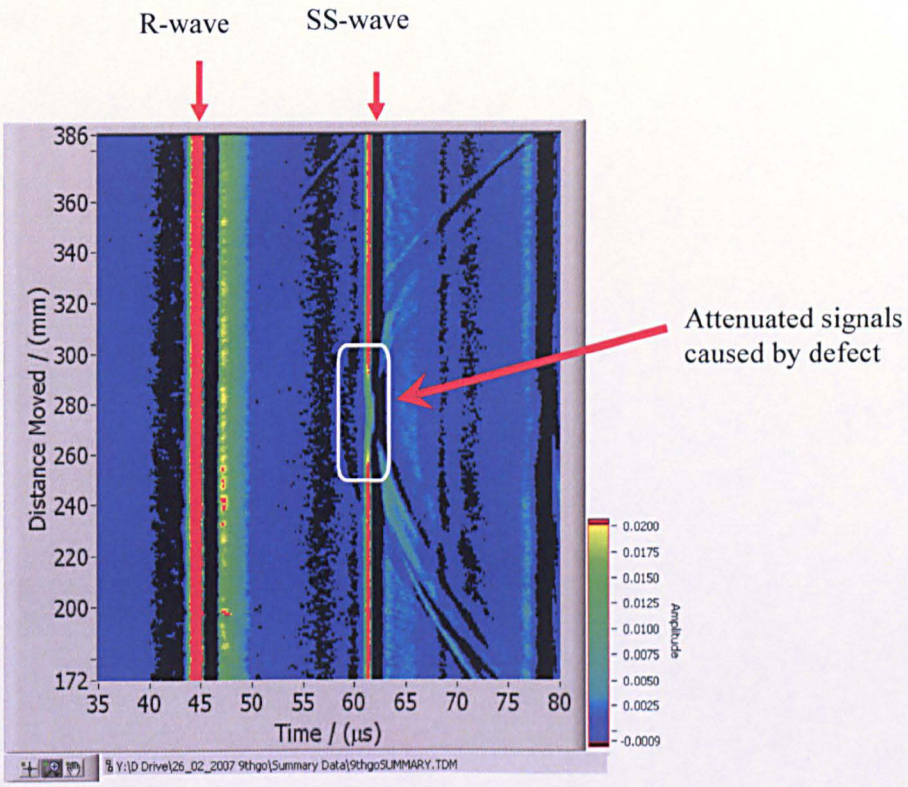

Fig. 30b: Magnified B-Scan showing the attenuation of the SS bulk wave.

11. LASER-EMAT ARRAYS

For on-line inspection, a single high energy, pulsed laser beam could be used as the ultrasonic generation source in conjunction with a number of EMAT sensors for detection. Therefore multiple EMATs could be used to cover the width of the steel being tested to inspect for defects that may lie in different orientations, along the surface and inside the steel.

As discussed in Section 6, for optimal surface crack detection, the EMAT coil should be as parallel as is reasonably possible to the crack and to the R-wave wavefront. It is well established that surface cracking in semis is predominately either longitudinal or transverse and that most surface defects can be at the two edges or in the middle of the semi[3]. Therefore, EMAT coils should be orientated to preferentially detect these types of defects. (In these different orientations, it is also possible to detect surface defects on the bottom and sides of the steel product, as well as some internal defects).

A plan view of an EMAT array is shown in Fig. 31. Here, the laser beam is targeted onto the middle of the billet and we assume that the pulse repetition frequency of the laser is suitably high to give complete coverage. Considering only surface defects on the top surface, from Fig. 31, EMAT #1 would detect any transverse defects in the middle of the billet. EMATs #2 and #3 would detect any longitudinal defects off-centre. They could also detect transverse defects as an additional signal reflected off the defect as illustrated in Fig. 5c. EMATs #4 and #5 could be used to detect corner cracking. Each of these five EMATs can also be used for finding internal defects.

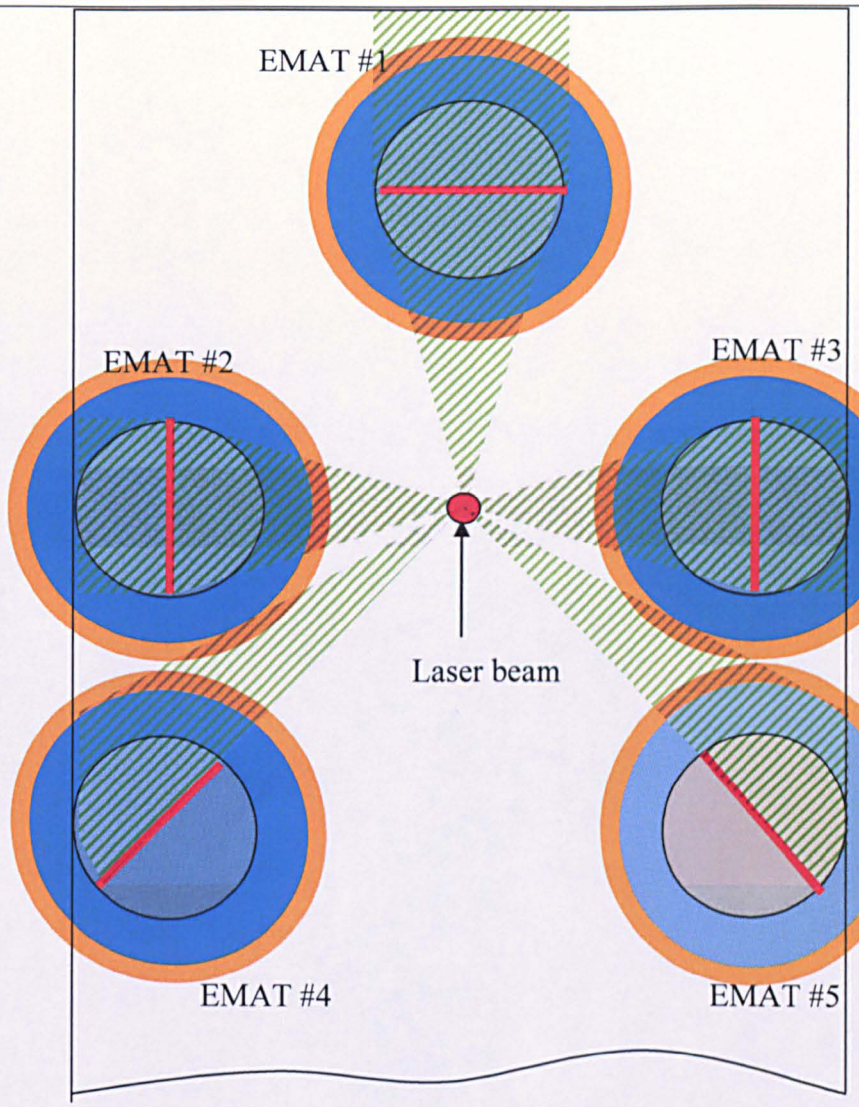

Fig. 31: Plan view showing an array of five EMATs
The red lines show the coil orientation. The shaded triangles show the areas of the billet that will be inspected. represents the paths of the surface waves, emanating from the laser beam, located in the middle of the array.

The size of defects that can be found are dependent upon how close the crack is to the laser beam impact point and the orientation of the EMAT coil. A relatively small defect would block the majority of the ultrasound emanating from the laser beam provided it was suitably close to the laser beam and the EMAT coil was oriented favourably towards the wavefront. The further away the same defect from the laser beam, the less of the wavefront the defect would block. Additionally, the ability to detect any defect is dependent upon its location in the steel. For instance, EMAT #1 would not detect a small transverse defect that was not in the middle of the steel. However, additional EMATs could be placed on either side of EMAT #1, with their coils oriented inwards, towards the laser beam allowing more transverse type defects to be detected.

A new EMAT holder was constructed for the pantograph system and tested using the automated trolley system. Here, an array of five EMATs were held in position above the steel and were used to inspect a steel billet. Figure 32 shows LabVIEW software written to acquire and stream up to six channels of A-Scan data to disk using the automated trolley system. Figure 32 shows five A-Scans from the five EMATs and one trigger signal from the photodiode detector. A trial was successfully conducted to prove that the PC system was fast enough to stream six channels of data to disk at once and that defects could be detected[6].

The only drawback to adding additional EMATs to the system would be the cost associated with additional high speed digitizer cards or multipliers to acquire the EMAT signals.

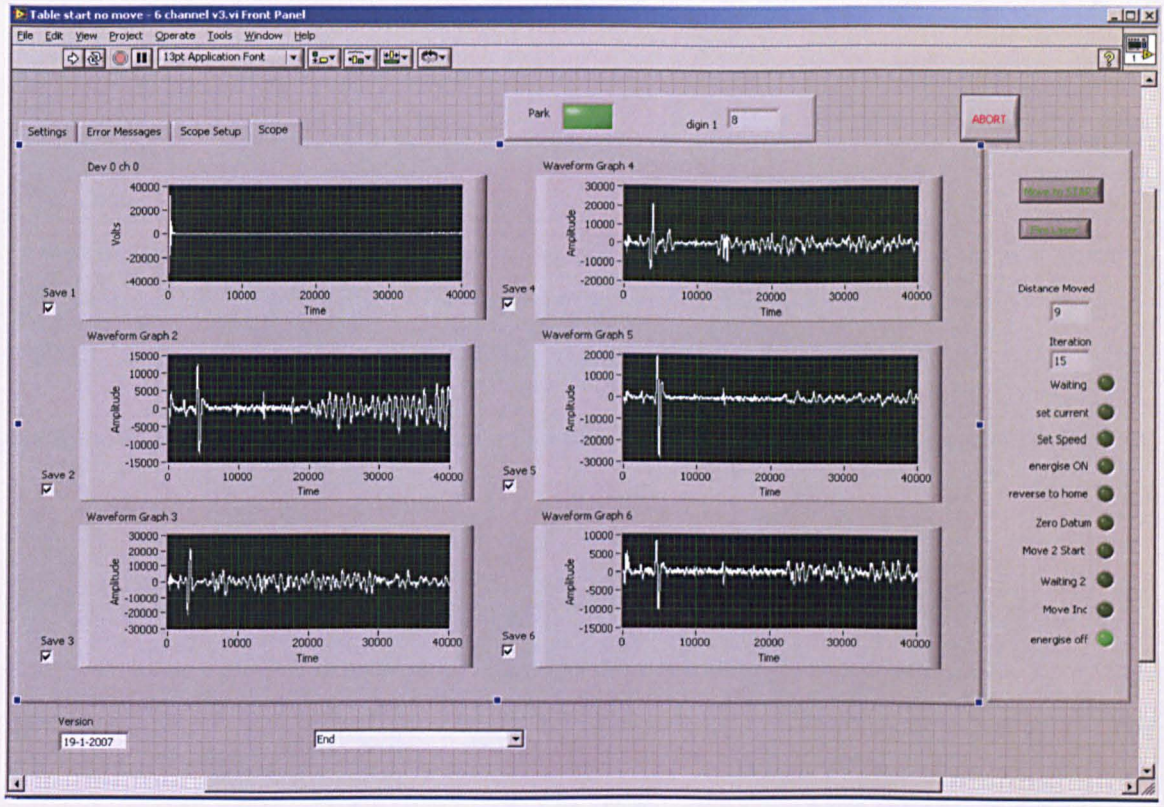

Fig. 32: Screen capture of the LabVIEW software used to acquire data from five different EMATs
(the top left graph shows the photodiode circuit, used for triggering).

12. INSTALLATION ON THE PILOT PLANT CONTINUOUS CASTER

In 2004, half way during the course of this project, the vertical billet caster in the Pilot Plant at Teesside Technology Centre was enhanced. To date, the caster has not been fully commissioned and therefore work on hot, moving steel was performed using a Pilot Rolling Mill. Some work, testing the robustness of EMATs on the original caster are contained in Engineering Doctorate Submission Number Four[6].

Figure 33 shows a photograph of the Laser-EMAT prototype installed on the new Pilot Plant continuous caster. The location is after the strand exits the last rolls from the roller straightener unit and before torch cut-off.

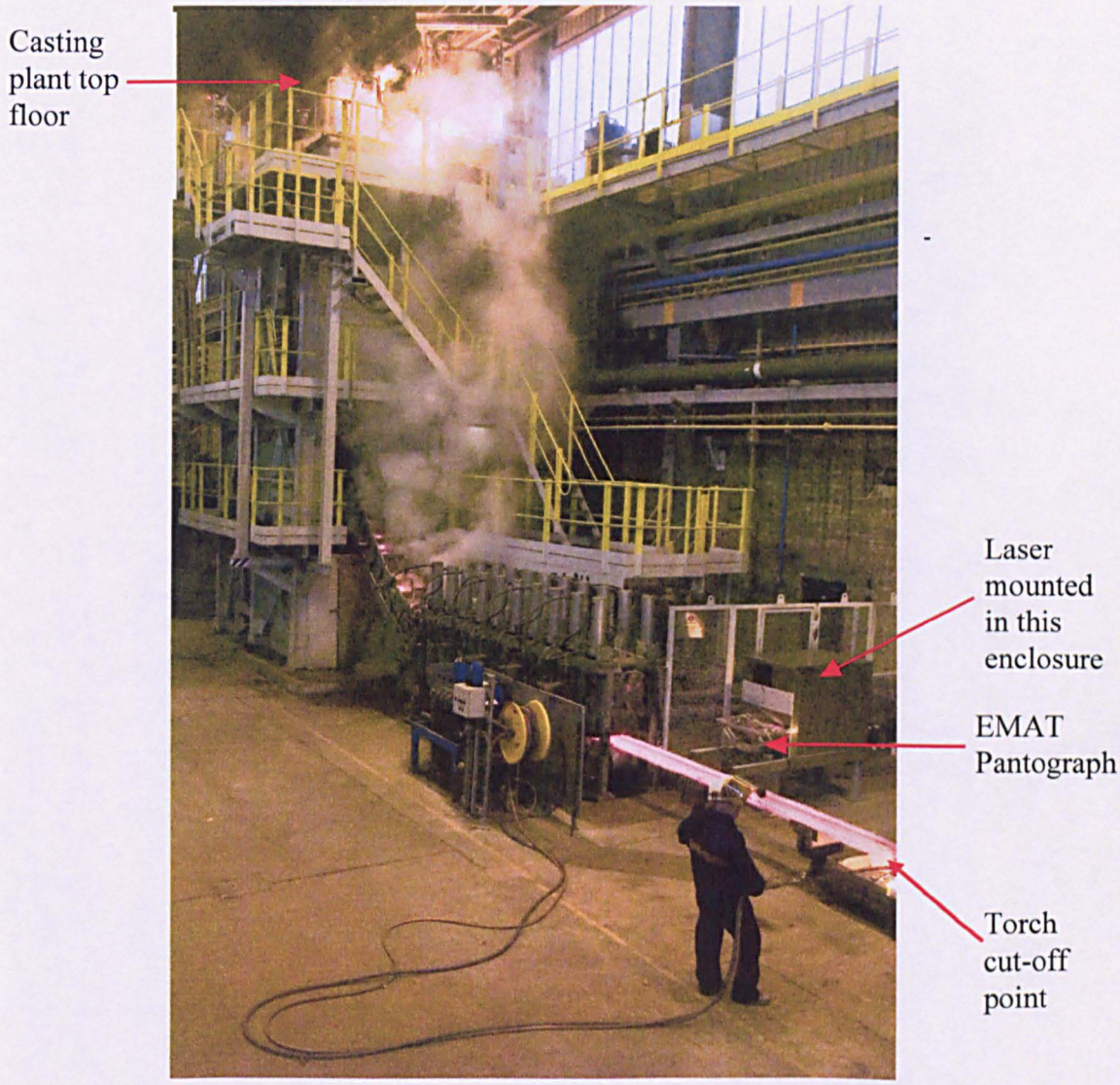

Fig. 33: View of the Laser-EMAT installation on the enhanced continuous caster at Teesside Technology Centre.

Work has started to prepare the Laser-EMAT system for on-line inspection. This new prototype will use the EMAT array developed as part of this project (Section 11) which will involve mounting the Laser-EMAT system on a sliding carriage system.

Figure 34 shows a photograph of the newly-designed carriage for mounting the EMAT pantograph and laser unit installed on the ground floor beside the torch cut-off point. This system allows the EMATs holder and laser to be kept positioned on the middle of the billet, even if the billet moves laterally during casting. This system uses the portable 532 nm laser mounted on the top of the frame, with the laser beam being steered by a prism and directed through a pantograph EMAT holder that is also attached to the same framework. The laser, power supply units and EMAT pantograph are all mounted on a telescopic slider system. Here, a cast iron wheel is mounted on the front of the framework and this is pushed against the as-cast product as it emerges from the soft reduction rollers. If the cast product moves from side to side, the slider will track it, keeping the laser and EMATs on the same position of the billet at all times. The system was designed to accommodate all the different billet dimensions that can be cast.

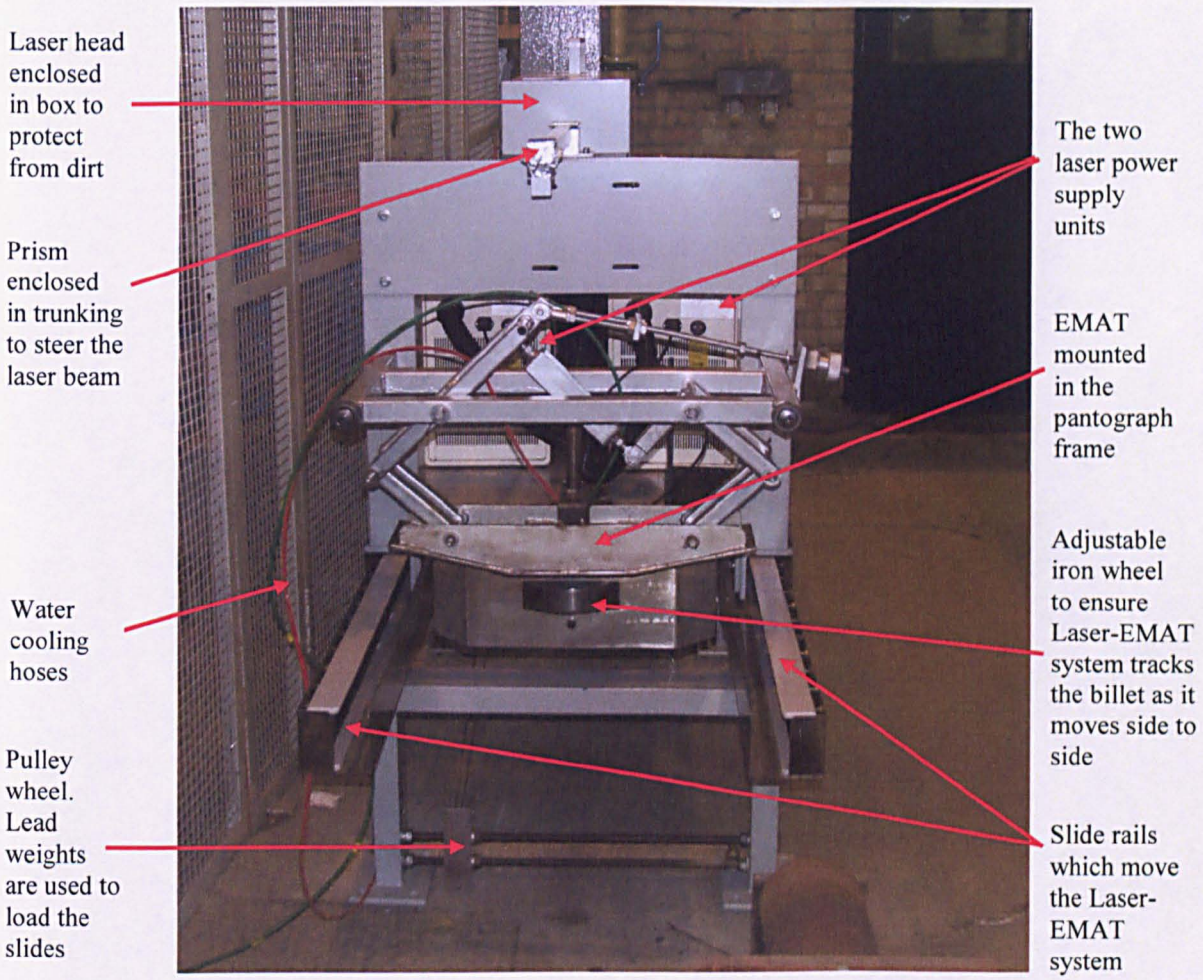

Fig. 34: Front view of the slider system with the laser mounted on top and EMAT held in pantograph (the protective covers, shown in Fig. 33 have been removed).

Figure 35 shows the Laser-EMAT system being tested on the caster. This trial was designed to ensure the water-cooled EMAT could survive prolonged proximity to hot moving steel and to ensure it was sufficiently mechanically robust. The Laser-EMAT system was also shrouded in heat resistant material so that the equipment would remain cool. Unfortunately the cast was aborted and only 2 m of steel was cast. The billet was therefore stopped directly underneath the EMAT sensor when it exited the straightener. The results from this trial showed that the slider system tracked the billet as it moved past and that the wheel did not stick. (Previous trials at room temperature also showed that the Laser-EMAT slider system could track the billet as it moved from side to side as a billet exited the straightener). Additionally, it was found that the laser cabinets and slider system did not overheat and that the radiated heat from the billet did not affect the prism or the prism trunking. This shows that the heat protection system used to shield the equipment from the heat of the billet will most probably work.

Fig. 35: View of the Laser-EMAT installation when heat shielded during a trial where the slider system and water-cooled EMAT sensor were being tested on hot steel from the caster.

Consideration has also been made regarding the safe use of laser systems. For practicality, casting plant operators cannot wear laser safety goggles. To solve the laser safety problem, the Class IV laser beam will be fully contained in a large box, in order to make the entire system Class 1. This means that from the roller straightener unit to the cut-off point will be fully enclosed with sheet metal to form a long tunnel and the equipment inside will be kept air cooled. The entry and exit points of this tunnel should therefore have protection surrounding the perimeter of the billet such that no reflected laser light can escape.

Different concepts to solve the problem to completely enclosing the laser beam were considered[6]. Here, the solution was to have a brush manufacturer to custom make a stainless steel draught excluder. This was tried and tested on the caster and this idea was therefore incorporated into the final enclosure. Pictures of the brush undergoing testing on the caster can be seen in Fig. 36.

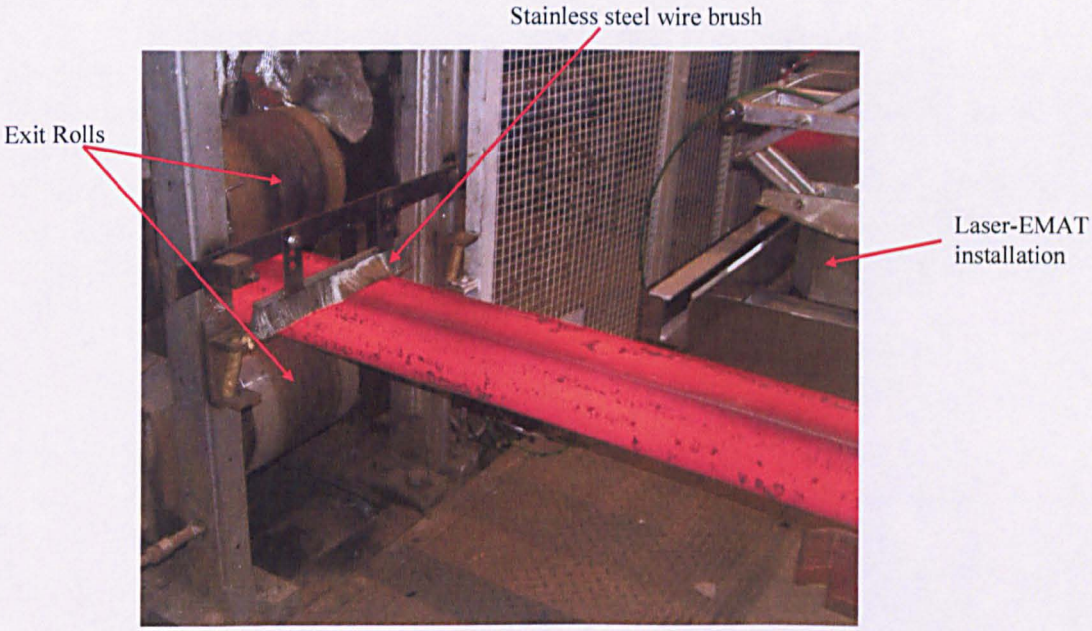

Fig. 36: View of the stainless steel wire brushes being tested.

13. RECOMMENDATIONS FOR THE FINAL LASER-EMAT SYSTEM

Although a prototype system has been developed to detect defects in steel, a significant amount of work must still be undertaken to optimise and ruggedise the system and to create a system that could be used in steel plants and marketed for other customers. Some of these recommendations for such a system are as follows:

- The laser system; A higher repetition laser rate laser should be used. This would lead to an increase in overall system resolution as more ultrasonic data per mm of product travel would be recorded. A higher energy, Q-Switched laser, with as large an energy output as possible should be used. A study should be conducted to compare different wavelengths of laser with pulse energy for high temperature applications. For slabs, a method to split the laser beam, or scan the laser beam across the slab width would need to be designed. One such concept can be seen in Fig. 37. Here, three arrays of EMATs could be used to cover the width of a slab. The majority of defects occur on the slab edges and in the middle of the face. These EMAT arrays could be multiplexed to share the same digitiser cards for signal acquisition. The path of the laser beam could be directed by mounting two rhomboid prisms in a holder that could be moved laterally very quickly using a servo motor system and a sliding rail. Smaller billets could be inspected with only one array of EMATs and blooms could be inspected with two arrays.

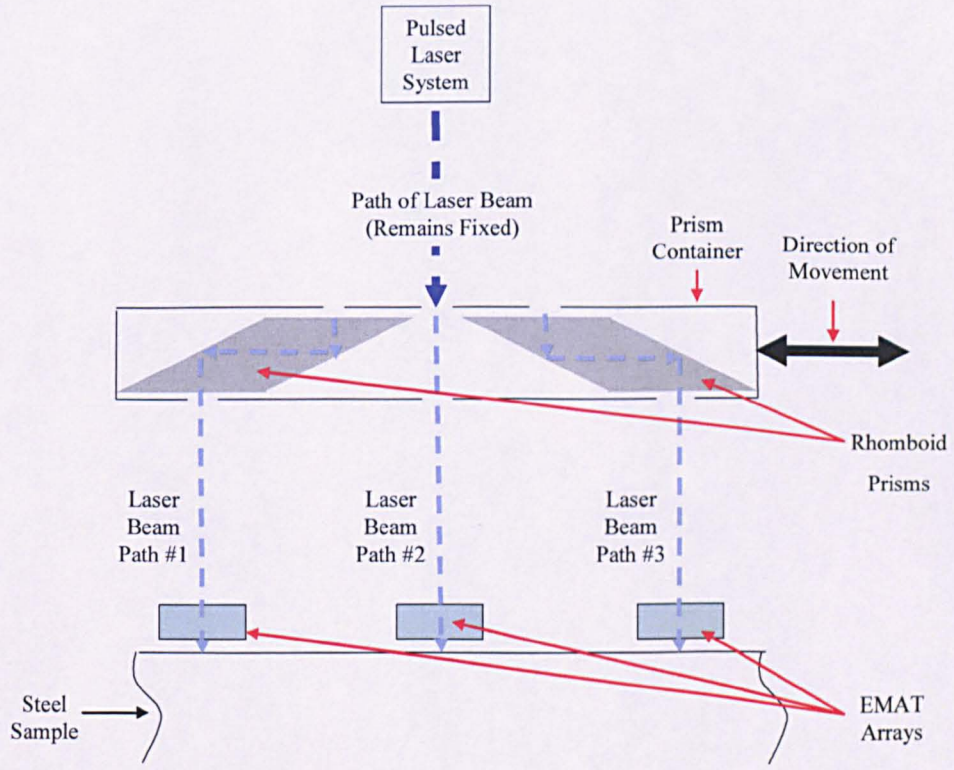

Fig. 37: Schematic diagram showing how prisms could be moved into the path of the laser to shift the beam direction either to the left or to the right so that different EMAT arrays can use the same laser beam.

- The EMATs; For slabs, three arrays of up to six EMATs could be mounted on the top of the slab - one array each for the left and right slab edges and one for the middle of the slab. The same laser could be used to generate signals in these three locations meaning that all the defects could be detected. A multiplexing system could be used to share channels on the high speed data acquisition cards as only one array would be in use at any one time. Top mounted EMAT arrays should also be capable of detecting surface defects on the slab bottom faces, as shown in Section 10.
- The software; Recent developments in hard disk technology and high speed data acquisition cards have made this project possible. It would not have been economically viable to record such high resolution signals in 2001 when the project started. What would be needed for a plant based system would be a computer with a dedicated, real-time operating system, which would be utilised solely for data collection. The new generation of dual-core processor technologies make it feasible to use one processor for data acquisition and the other for data analysis in real-time. It should therefore be possible to save only the "regions of interest", i.e. only save data when a defect is present. By examining the ultrasonic signals, it should be possible to determine the location and size of the defects.
- An FPGA (Field Programmable Gate Array) could be used to process and analyse the data. For instance, this system could remove extraneous data from the raw EMAT signals and perform calculations to ensure that only the data from regions that contained defects were then sent to disk. This means that the requirements for constant disk access on a computer system, running 24/7 would be reduced.
- The plant system; The final system would have to be very robust. The EMATs would need to be very well protected to keep loose scale from damaging them. The entire system would need to be enclosed for laser safety. Any moving parts would require shielding from grit. The high temperature would require the use of low thermal conductivity materials and/or effective cooling to ensure system longevity.

14. MAIN INNOVATIONS

I. Identified a suitable system with the potential for on-line inspection

At the start of the EngD project, a problem regarding the quality assessment of as-cast steel semis was identified (Section 2)[1]. Here, it was evident that having an on-line inspection system would help to increase process efficiency and reduce costs. One of the main advantages for on-line inspection would be to have a real time system alerting operators to quality issues, i.e. whether or not the steel being manufactured contained any surface or internal defects. Were such a system to exist, it would enable operators to rectify the cause of the problem (Section 3). The importance placed on such a system is further reinforced by the letter of support from the Technical Director of Corus, Scunthorpe Cast Products (Appendix 1). In order to find the solution to this problem, the literature was reviewed and a recommendation for an on-line system was made (Section 4)[4,5]. The Laser-EMAT system was selected because it is non-contact and was thought to be suitable for operating in the harsh environment of the continuous casting plant, where steel can be in excess of 600°C and moving at speeds up to 5 m/min. Because a Laser-EMAT system was not available off-the shelf, to implement the solution, significant research work was undertaken to create a Laser-EMAT system that was successfully used to find a defect on a hot, moving steel billet sample in the Pilot Rolling Mill (Section 9)[6]. Further recommendations for installing a prototype Laser-EMAT system on a continuous caster are given in Section 12.

II. Developed a laboratory-based system into a system ready for on-line inspection

A laboratory based trolley system was designed and built to test moving steel samples at room temperature (Section 8)[6]. Several aspects made it possible to enable a Laser-EMAT system to inspect steel billet samples automatically. This trolley system can be considered as one innovation, involving many smaller parts which were important in implementing a system suitable for inspecting hot, moving steel. One major innovation was the creation of a pantograph holder which enabled an array of EMATs to be held parallel and with a near constant stand-off above the steel sample (Section 8.1). Another was writing software and building hardware capable of saving significant quantities of data to disk from multiple EMAT sensors (Section 8.2). By integrating these different technologies, it was possible to create an on-line laboratory system that could move steel samples, acquire data from an array of EMATs, fire the laser system and then analyse the data at a later stage (Section 9.3). This work demonstrated the potential for using a Laser-EMAT system for inspecting moving steel for defects and this led to further trials moving the steel on the Pilot Rolling Mill and subsequently to inspecting hot, moving steel on the same mill (Section 9.6).

III. Taking measurements on hot, moving steel

This project demonstrated that EMAT sensors could be designed to be robust and water-cooled to ensure the permanent magnet used to construct the EMAT remained below its Curie Point such that ultrasonic measurements could be taken (Section 7)[6]. Initially the water-cooled EMAT was tested on stationary steel samples and ultrasonic measurements were recorded. When confidence was gained using the Laser-EMAT system to inspect moving samples at room temperature, the EMAT was then demonstrated successfully to work on hot, moving steel

and ultrasonic measurements were taken on a steel billet, highlighting the presence of a defect (Section 9.6).

IV. Developing a Laser-EMAT System with the potential for being installed on-line.

Due to the Pilot Plant continuous caster not having been fully commissioned, work on hot, moving steel was performed using a Pilot Rolling Mill. The rolling mill helped to identify problems that were subsequently solved and allowed recommendations to be made for the final prototype design for the Pilot Plant Continuous Caster (Section 12). This enabled the design of an enclosure for the Laser-EMAT system that could contain the high powered laser beam meaning operators would not need to wear laser safety goggles. Currently, this system is being constructed in preparation for the time when the Pilot Plant Continuous Caster can be used reliably and is fully commissioned. It is hoped to validate the Laser-EMAT system by finding defects that have been induced deliberately in the steel. The results from the ultrasonic signals would be analysed and compared to manual, visual inspection of the steel surface and metallurgical samples that have been sulphur printed. After the Laser-EMAT system has been demonstrated sufficiently a prototype would be installed on a commercial continuous caster.

15. CONCLUSIONS

A solution to a manufacturing problem whereby operators did not know the quality of steel being produced until several days after continuous casting was found. The resulting implementation was an automated system for testing billets and producing B-Scans displaying the location of defects was designed and constructed. This system which exhibited a high degree of automation and was controlled using LabVIEW software was designed and constructed.

Through detailed inspection of the billet at room temperature and under controlled laboratory conditions, it was possible to test the same billet on a pilot scale mill. The Laser-EMAT system was demonstrated successfully to find a defect on hot, moving steel using the Pilot Rolling Mill. A prototype Laser-EMAT system has been installed on the ground floor level of the Pilot Plant Continuous Caster. Preliminary work, demonstrating how the system can remain centred on the billet during casting and be shielded from the heat has been successful. More work needs to be done to develop a system to completely enclose the pulsed laser beam and to develop a prototype system that could identify defects and feed back the information to the operators during continuous casting. The building blocks for such a system have been proven feasible as part of this project.

16. LIST OF PUBLISHED PAPERS RESULTING FROM THE ENGINEERING DOCTORATE PROJECT

Baillie, I, Griffith, P, Jian, X, Dixon, S: 'Implementing an ultrasonic inspection system to find surface and internal defects in hot, moving steel using EMATs', Insight, Vol. 49, No. 2, Feb 2007

Jian, X, Baillie, I, Dixon, S: 'Steel billet inspection using Laser-EMAT system', J Phys D: Appl Phys, Vol. 40, 2007, pp1501-1506

Jian, X, Dixon, S, Edwards, R, Morrison, J: 'Integrity evaluation of steel products using EMATs', J Phys D: Appl Phys, Vol. 40, 2007, pp300-304

Jian, X, Dixon, S, Baillie, I, Edwards, R.S, Morrison, J, Fan, Y: 'Shear wave generation using a spiral electromagnetic acoustic transducer', Applied Physics Letters, Vol. 89, Dec 2006

Dixon S, Edwards C, Palmer S B: 'A laser-EMAT system for ultrasonic weld inspection', Ultrasonics Vol. 37, pp273-281, 1999

17. REFERENCES

1. Baillie I: 'An introduction to the defects caused during the continuous casting of steel and the need to detect them on line'. Engineering Doctorate Portfolio Submission Number 1, November 2003

2. Knox T J: 'Measurement and analysis - a basis for steel quality and customer confidence', Iron and Steelmaking, Vol. 18, No 3, pp196-200, 1991

3. Irving W R: 'Continuous casting of steel', pub. The Institute of Materials, ISBN 0-901716-53-7, 1993

4. Baillie I: 'Potential systems to inspect the surface and internal structure of as-cast semis', Engineering Doctorate Portfolio Submission Number 2, March 2005

5. Baillie I: 'The potential use of non-contact ultrasonics for the on-line inspection of semis', Engineering Doctorate Portfolio Submission Number 3, November 2005

6. Baillie I: 'Steps toward an automated prototype system for inspecting hot, moving steel', Engineering Doctorate Portfolio Submission Number 4, August 2007

7. Zangh L, Thomas B G: 'State of the art in evaluation and control of steel cleanliness', ISIJ International, Vol. 43, No 3, pp271-291, 2003

8. Wadley H N G, Norton S J, Mauer F, Droney B: 'Ultrasonic measurement of internal temperature distribution', Phil. Trans. R. Soc. Lond. A 320, pp341-361, 1986

9. Corus Teesside Cast Products, Work Instruction, Document Number HSUL-4NAHYA, 31/03/2003

10. Baillie I, Griffith P, Smith A W, McDonald M, Sancho L, Diaz J, Colla V, Sgarbi M: 'SURFQUALDEV: The measurement and prediction of surface quality by new developments in EMATs and scarfing and the effect of scarfing on surface defects through the mills', Final Research Fund for Coal and Steel (RFCS) Report, EU Reference R679, 2007

11. 'Detection des defaults de surface et sous-cutanes sur les billettes chaudes de coulee continue par courants de Foucault' ('Default detection on the surface on hot continuously cast billets'), ECSC Report, European Steel and Coal Commission EUR 15583 FR

12. Patrick B: 'Visit to Solmer to assess slab crack detection system and observe a computer slab quality prediction scheme', British Steel Internal Report T/CR/V/1396/16/85/D, 1985

13. Mercklé J, Sauter D, Rayot J, Lajournade J-B, Watrinet J-M: 'Intelligent sensing for non-destructive testing using eddy currents', NDT International, Vol. 23, No. 6, Dec 1990

14. Savidge D H: 'Proposal for the development of the MIDAS billet inspection equipment at CES Aldwarke Works', Corus Internal Report SL/IN/TN/S2743/1/00/D, 2000

15. Sancho L F, Falessi R, Diez A: 'On-line slab surface inspection in continuous casting using novel conoscopic holography (SURFIN C.C.)', ECSC Report EUR 20461, 2002

16. Sancho L F, Obeso F, Alvarez I, Diez A, Sirat G, Falessi R: 'Novel on-line surface quality control for hot slabs in continuous casting', La Revue de Metallurgie - ATS - JSI 2001, pp226-227, 2001

17. Sancho L F, Obeso F, Alvarez I, Diez A, Sirat G, Falessi R: 'On-line slab surface inspection based on conoscopic holography', SMEA Conference and Exhibition - Automation in Metals Processing, 27th-28th June 2002, University of Sheffield

18. Edwards R S, Dixon S, Jian X: 'Depth gauging of defects using low frequency wideband Rayleigh waves', Ultrasonics, Vol. 44, pp93-98, 2006

19. Idris A, Edwards C, Palmer S B: 'Acoustic wave measurements at elevated temperature using a pulsed laser generator and an electromagnetic acoustic transducer detector', Nondestr. Test. Eval, Vol. 11, pp195-213, 1994

20. Rohani Md S: 'The development of non-contact laser and EMAT ultrasound measurement systems for hot steel', PhD Thesis, Department of Physics, The University of Warwick, 1996

21. Scruby C B, Drain L E: 'Laser ultrasonics techniques and applications', pub. Adam Hilger ISBN 0-7503-0050-7, 1990

22. Murray P R, Dewhurst R J: 'Application of a laser/EMAT system for using shear and LS mode converted waves', Ultrasonics, Vol. 40, pp771-776, 2002

23. Nadeau F, Hutchins D A: 'A study of the interaction of surface waves with slots using non-contact laser generation and detection of ultrasound', IEEE Ultrasonics Symposium, 1984.

24. Dewhurst R J, Edwards C, Palmer S B: 'Non-contact detection of surface-breaking cracks using a laser acoustic source and electromagnetic acoustic receiver', Appl Phys Lett, Vol. 39, No 7, pp274-376, 1986

25. Dixon S, Edwards C, Palmer S B: 'A laser-EMAT system for ultrasonic weld inspection', Ultrasonics, Vol. 37, pp273-281, 1999

26. Boonsang S, Dewhurst R J: 'Enhancement of laser-ultrasound/electromagnetic-acoustic transducer signals from Rayleigh wave interaction at surface features', Applied Physics Letters, Vol. 82, No 19, 2003

27. Bernstein J R, Spicer J B: 'Hybrid laser/broadband EMAT ultrasonic system for characterizing cracks in metals', J. Accoust. Soc. Am, Vol. 111, No 4, pp1685-1691, 2002

28. Hopko S N, Ume I C: 'Laser ultrasonics: simultaneous generation by means of thermoelastic expansion and material ablation', Journal of Non-destructive Evaluation, Vol. 18, No 3, pp91-98, 1999

29. Hirao M, Ogi H: 'EMATs for science and industry: Non-contacting ultrasonic measurements', Kluwer Academic Publishers, ISBN 1-4020-7494-8, 2003

30. Mason E P(Ed), Thurston R N(Ed): 'Physical acoustics, 'Principles and methods', Academic Press, Volume XIV, 1979

31. Mason E P(Ed), Thurston R N(Ed): "Physical acoustics, 'Principles and methods', Academic Press, Volume X, 1973

32. Dewhurst R J, Edwards C, McKie A D W, Palmer S B: 'A remote laser system for ultrasonic velocity measurement at high temperatures', J Appl. Phys, Vol. 63, No 4, pp1225-1227, 1988

33. Tittmann B R, Aslan M: 'Ultrasonic sensors for high temperature applications', Japanese Journal of Applied Physics, Vol. 38, pp3011-3013, 1999

34. Scruby C B, Moss B C: 'Non-contact ultrasonic measurements on steel at elevated temperatures', NDT&E International, Vol. 26, No 4, pp177-188, 1993

35. Wadley H N G, Norton S J, Mauer F, Droney B: 'Ultrasonic measurement of internal temperature distribution', Phil. Trans. R. Soc. Lond. A 320, pp341-361, 1986

36. Rogers C D, Droney B E, Tith J M, Wadley H N G: From the Conference Proceedings of the 26th Mechanical Working and Steel Processing Conference; 'Detection of pipe and porosity in hot steel slabs, blooms and billets', pp283-287, Chicago, Illinois, October 1984

37. Oberhoff D, Eberle, Meyer J: 'Pilot plant for contactless internal and surface on-line inspection of stainless steel strips', ECSC Draft Final Report 1/7/99 - 31/12/02, 2003

38. Coen G, Lost E, Oberhoff D, Lampey H: 'HeiBprufung von StrangguBbrammen mittels elektromagnetischer Ultraschallprufkopfe' ('Hot inspection of continuously cast slabs using electromagnetic ultrasonic test probes'), ECSC Report EUR 15173 DE, ISBN 92-826-9513-1, 1995

39. Coen G, Kroos J: 'Entwicklung einer Ultraschallprototypanlage zur Prufung von heiBen StrangguBbrammen' ('EMATs tested in a steel works, on a continuous casting machine'), ECSC Report EUR 18372 DE, ISBN 92-828-4488-9, 1993

40. Neumann N: 'Application de capteurs electromagneto-acoustiques aux brames chaudes coulees en continu' ('Surface defect detection on continuously cast slabs, using EMATs') ECSC Report EUR 13479 FR, 1990

41. Kaye G W C, Laby, T H: 'Tables of physical and chemical constants', 15th Edition, pub. Longman Scientific & Technical, ISBN 0-470-20662-4, 1986

42. Dubois M, Militzer M, Moreau A, Bussiere J F: 'A new technique for the quantitative real-time monitoring of austenite grain growth in steel', Scripta Materialia, Vol. 42, No. 9, 2000

43. TT Electronics Brochure "Permanent mangnets", from MMG MagDev Limited.

44 Bentley J P: 'Principles of measurement systems', 3rd Edition, pub. Addison Wesley Longman Ltd, 1997, ISBN 0-582-23779-3, p156

45 Jian X, Baillie I, Dixon S: 'Steel billet inspection using laser-EMAT system', J. Phys. D:Appl. Phys., Vol. 40, pp1501-1506, 2007

APPENDIX 1

To Whom It May Concern

Corus Construction & Industrial
PO Box 1
Brigg Road
Scunthorpe
North Lincolnshire DN16 1BP
United Kingdom

T +44 (0) 1724 404040
T 01724 402888 (direct)
F 0870 9031243 (direct)
chris.elliot_BMT@corusgroup.com

14 August 2007

To Whom It May Concern:

Semi-finished product integrity (in the as-cast condition) is a critical component of the integrated steel processing value chain. Producers strive to develop operational practices which produce defect-free material via a thorough understanding of the interaction of process parameters and metallurgical characteristics; failing this, a variety of techniques are used to either detect, or predict, the extent of surface and subsurface defects that may create quality issues and losses in subsequent processes.

If a system could be developed and installed to inspect semis automatically during the continuous casting process, then significant cost savings could be made. This is a challenging task as the inspection system would be expected to find both surface and internal defects in semis at elevated temperature, when the steel is being continuously cast.

The Laser-EMAT system currently being developed at Corus Teesside Technology Centre, has been jointly supported and funded by two Corus Business Units; Corus Construction & Industrial (Scunthorpe) and Corus Strip UK (Port Talbot). Partial funding has also been made from the European Research Fund for Coal and Steel (ERFCS). The Corus Project Leader is undertaking this project as part of the Engineering Doctorate Scheme at The University of Warwick.

The envisioned advantages to the Business Units are thus:

- 'Real time' feedback could be given to casting operators enabling the casting process to be interrupted if defects are severe or modifications made on-line to rectify situations which may be

Corus UK Limited
Registered Office 30 Millbank
London, SW1P 4WY
Registered in England No. 2280000

causing defects, e.g. SEN or mould powder problems.

- An on-line system could be used to guarantee the quality of as-cast semis and their suitability for downstream processing within Corus or prior to dispatch to external customers. Therefore semis would not be subjected to value-added processes when they should be scrapped or downgraded for other applications should they contain any defects.
- Currently some steel grades are mandatory scarfed, regardless of whether or not they contain any defects. The system would identify semis which did not need scarfing and this could give significant yield and energy savings.
- The need for "visual" inspection, involving operators inspecting hot steel in slab yards would be reduced significantly.
- An inspection system could be linked into plant "quality tracking" software allowing managers to track what happens to products when they contain certain types of defects.

To date, the work performed on the Laser - EMAT system has been rigorous from both a metallurgical and engineering viewpoint. Results to date indicate there is genuine potential to develop the characterisation technology into a full industrial - scale online monitoring system.

Progress on the project has been pleasing and has maintained the faith and support of the Corus business units involved throughout - a commendable piece of work.

Yours sincerely

Chris Elliot
Director Technical